Ultrasensitive and versatile hydrogen peroxide sensing via fluorescence quenching

Jenisha John Peter,[†] *Nathaniel Chennattuparambil Roy,*[†] *Flavio Grynszpan, Mindy Levine*

[†] These authors contributed equally to this work.

TABLE OF CONTENTS

Materials and Methods……S3

Experimental Procedures……S4

Synthetic procedures……..S4

Solution-state experiments…….S5

Filter paper-based experiments……..S9

^{1}H NMR titration experiments…….……..……..…….S10

Summary Tables…..……..……..…….S11

Solution-state experiments……..……..……...S11

Filter paper-based experiments……S19

Summary Figures…….....S21

Synthesis figures……..S21

Solution-state experiments……...S24

Filter paper-based experiments…….....S32

High resolution mass spectrometry experiments……..S34

^{1}H NMR titration experiments……..……S35

References…….S40

I. MATERIALS AND METHODS

All reagents were purchased from Tzamal Medical Group (Petah Tikva, Israel), Holland Moran Ltd. and Sigma Aldrich and were used without further purification. All organic solvents used were HPLC grade and were dried over activated molecular sieves (3 Å or 4 Å) prior to use. NMR solvents were purchased from Thermo Scientific Chemicals and dried over activated molecular sieves (3 Å or 4 Å) prior to use. Ultra-pure water was obtained using a Milli-Q® machine, in which water is processed through the QPAK® purification cartridge to reach a resistivity of 18.2 MΩ•cm (25°C) and a TOC value below 5 ppb. All UV-Visible absorbance spectra were acquired on a Jasco V-750 UV-visible spectrophotometer, using a 10 mm path-length quartz cuvette. Fluorescence spectra were recorded on a Varian Cary Eclipse fluorescence spectrophotometer, with emission recorded at a 90^{o} angle relative to the excitation source. ^{1}H NMR spectra were obtained using a Bruker Avance III spectrophotometer operating at 400 MHz. The pH values of aqueous solutions were recorded on a Mettler Toledo Education Line pH meter. All of the high-resolution mass spectra (HRMS) were measured in positive ionization mode using a Waters Micromass Quattro Micro instrument, which was equipped with an electrospray ionization source and Waters 2795 and 996 PDA detectors. The measurements were carried out using a MIRacle^{TM} Single Reflection ATR Accessory from PIKE Technologies, without any sample processing. All fluorescence spectra were integrated vs. wavenumber on the X-axis using OriginPro 2020. All curve fitting was done using OriginPro curve fitting options (either linear or non-linear curve fitting, as applicable). All colorimetric analysis was done using freely available ImageJ software (https://imagej.net/ij/index.html).

II. EXPERIMENTAL PROCEDURES

a. *Synthetic procedures*

i. Synthesis of compound **1**:

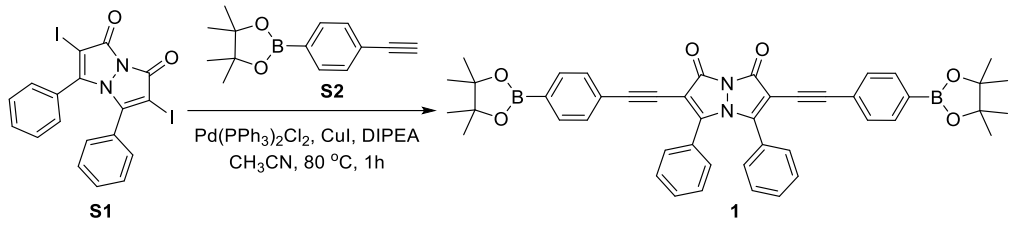

Figure S1. Synthesis of compound **1**

syn-(Ph,I) Bimane (compound **S1**) was prepared following literature-reported procedures.[1] To prepare compound **1**, compound **S1** (100 mg, 0.28 mmol, 1.0 equiv.) was dissolved in acetonitrile (200 mL) under a nitrogen atmosphere at room temperature, and 4-ethynylphenylboronic acid pinacol ester **S2** (140 mg, 0.61 mmol, 2.2 equiv.), bis(triphenylphosphine)palladium (II) chloride (20 mg, 0.028 mmol, 0.10 equiv.), cuprous iodide (2.7 mg, 0.014 mmol, 0.05 equiv.) and *N,N*-diisopropylethylamine (0.48 mL, 2.8 mmol, 10 equiv.) were added. The reaction mixture was stirred at 80 °C for 1 hour and the solvent was then evaporated under reduced pressure. The resulting crude product was purified via column chromatography using 5% ethyl acetate in dichloromethane (*vol/ vol*) as an isocratic eluent to obtain compound **1** in 67% yield (138 mg) as an orange solid. ^{1}H NMR ($CDCl_3$, 400 MHz): δ = 7.70 (d, *J* = 8.0 Hz, 2 H, Ar-H), 7.35 (d, *J* = 8.1 Hz, 2 H, Ar-H), 7.32-7.30 (m, 2 H, Ar-H), 7.23 (d, *J* = 4.4 Hz, 1 H, Ar-H), 7.17-7.13 (m, 2 H, Ar-H), 1.33 (s, 12 H, 2(-Me)2) ppm; ^{13}C NMR ($CDCl_3$, 101 MHz): δ = 157.29, 151.83, 134.95, 131.56, 131.20, 129.63, 128.90, 128.61, 125.77, 125.35, 104.59, 98.39, 84.46, 25.32 ppm; HRMS: m/z calcd. for $C_{46}H_{42}B_2N_2O_6$: 741.3322; found: 741.3322 [$M+H^+$].

ii. Synthesis of compound **2**:

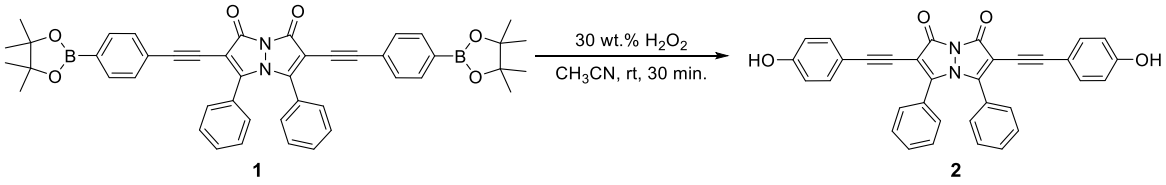

Figure S2. Synthesis of compound **2**

Compound **1** (110 mg, 0.148 mmol, 1.0 equiv.) was dissolved in acetonitrile (100 mL) in a round bottom flask, followed by the addition of 30% H_2O_2 (w/v, 37 µL, 0.325 mmol, 2.2 equiv.). The reaction mixture was stirred at room temperature for 30 minutes, followed by removal of the solvent under reduced pressure. The crude product was purified by reverse phase HPLC (eluent: 60% acetonitrile: 40% water) to yield bimane **2** as a red solid (15 mg, 21% yield). ^{1}H NMR (DMSO-d_6, 400 MHz): δ = 9.98 (s, 1 H), 7.35 – 7.28 (m, 3 H), 7.21 – 7.14 (m, 4 H), 6.74 (d, *J* = 8.7 Hz, 2 H) ppm; ^{13}C NMR (DMSO-d_6, 101 MHz): δ = 132.88, 129.12, 127.78, 125.27, 115.80 ppm; HRMS: m/z calcd. for $C_{34}H_{20}N_2O_4$: 521.1501; found: 521.1486 [$M+H^+$].

b. Solution-state experiments

i. Water vs. hydrogen peroxide response comparison

Steady-state UV-visible spectroscopy experiments: A stock solution of compound **1** in acetonitrile ([**1**] = 10 μM) was prepared, and the UV-visible absorption spectrum of the solution was recorded from 200-800 nm. Solutions of compound **1** were also prepared in the presence of increasing concentrations of H_2O_2 ([H_2O_2] = 0.029 M – 0.676 M; [**1**] = 10 μM), and the UV-visible spectrum of each solution was recorded. Solutions of compound **1** were also prepared in the presence of increasing concentrations of H_2O ([H_2O] = 0.18 M – 4.26 M; [**1**] = 10 μM), and the UV-visible spectrum of each solution was recorded. The results reported herein represent an average of at least three independent trials.

Steady-state fluorescence spectroscopy experiments: A stock solution of compound **1** in acetonitrile ([**1**] = 10 μM) was prepared, and the fluorescence emission spectrum of the solution was recorded from 460-800 nm ($\lambda_{excitation}$ = 450 nm; excitation and emission slit widths = 2.5 nm). Solutions of compound **1** were also prepared in the presence of increasing concentrations of H_2O_2 ([H_2O_2] = 0.029 M – 0.676 M; [**1**] = 10 μM), and the fluorescence spectrum of each solution was recorded under the same experimental conditions (($\lambda_{excitation}$ = 450 nm; excitation and emission slit widths = 2.5 nm). Solutions of compound **1** were also prepared in the presence of increasing concentrations of H_2O ([H_2O] = 0.18 M – 4.26 M; [**1**] = 10 μM), and the fluorescence spectrum of each solution was recorded under the same experimental conditions (($\lambda_{excitation}$ = 450 nm; excitation and emission slit widths = 2.5 nm). The results reported herein represent an average of at least three independent trials.

ii. Limit of detection experiments:

The initial sample was prepared by diluting a solution of compound **1** in acetonitrile ($[\mathbf{1}]_{initial}$ = 50 μM; $[\mathbf{1}]_{final}$ = 10 μM).

The diluted solution was transferred to a quartz cuvette, and excited at 450 nm using a Varian Cary Eclipse fluorescence spectrometer. The excitation and emission slit widths were fixed at 2.5 nm. The fluorescence emission spectrum was collected between 460 and 800 nm. Each fluorescence measurement was repeated six times.

A solution of 0.5 nM of H_2O_2 in water was diluted with compound **1** (3 mL) to achieve a final concentration of 0.005 nM H_2O_2 and the solution was manually stirred. The UV-visible absorbance spectrum of the solution was collected between 200 and 700 nm. The steady-state fluorescence emission spectrum was collected by exciting the solution at 450 nm, and recording the emission between 460 nm and 800 nm. All measurements were repeated six times.

The above step was repeated five times to get final hydrogen peroxide concentrations of 0.01 nM, 0.05 nM, 0.1 nM, and 0.15 nM. In all cases, the solution was excited at 450 nm and the fluorescence emission spectrum was recorded between 460 and 800 nm.

We plotted the concentration of hydrogen peroxide (in nM) on the X-axis, and a variety of measured output data on the Y-axis (integrated UV-visible absorbance spectra; intensity of absorbance at 455 nm, integrated fluorescence emission spectra, and intensity of fluorescence emission at 534 nm). The equations for the best linear fit for each data set were determined.

The limit of detection of the blank (LOD_{blank}) and limit of quantification of the blank (LOQ_{blank}) were calculated using the following equations:

$$LOD_{blank} = Average_{blank} + 3 * SD_{blank} \quad \text{(Eq. S1)}$$

$$LOQ_{blank} = Average_{blank} + 10 * SD_{blank} \quad \text{(Eq. S2)}$$

where $Average_{blank}$ represents the average measured value of the repeated trials of the sample without any analyte (i.e., hydrogen peroxide), and SD_{blank} represents the standard deviation of those measurements.

For each category of output data, we plugged the LOD_{blank} value into the best linear fit equation as the Y-value, and solved for the X-value. This value represents the limit of detection, measured as the concentration of hydrogen peroxide in μM.

For each category of output data, we plugged the LOQ_{blank} value into the best linear fit equation as the Y-value, and solved for the X-value. This value represents the limit of quantification, measured as the concentration of hydrogen peroxide in μM.

iii. Solution-state colorimetric analysis

Colorimetric analysis of H_2O_2: 1 mL of an acetonitrile solution of compound **1** ([**1**] = 10 μM) was added to 10 different vials. Varying amounts of an acetonitrile solution of H_2O_2 ([H_2O_2] = 500 mM) were then added to the vials containing solutions of compound **1**, to achieve the following H_2O_2 concentrations: 0 mM, 10 mM, 30 mM, 60 mM, 90 mM, 120 mM, 150 mM, 180 mM, 210 mM, 240 mM, 270 mM, and 300 mM. The vials were mixed by hand, and allowed to sit at room temperature for five minutes prior to being photographed under ambient light and under 365 nm excitation (using a hand-held TLC lamp). Colorimetric analysis of the resulting photographs was conducted using ImageJ software. The results reported herein represent an average of three independent trials.

Colorimetric analysis of water: The same procedure was repeated using a 500 mM solution of water in acetonitrile. This solution was added to vials containing 1 mL of a solution of compound **1** in acetonitrile ([**1**] = 10 μM), to achieve the following water concentrations: 0 mM, 10 mM, 30 mM, 60 mM, 90 mM, 120 mM, 150 mM, 180 mM, 210 mM, 240 mM, 270 mM, and 300 mM. The vials were mixed by hand, and allowed to sit at room temperature for five minutes prior to being photographed under ambient light and under 365 nm excitation (using a hand-held TLC lamp). Colorimetric analysis of the resulting photographs was conducted using ImageJ software. The results reported herein represent an average of three independent trials.

iv. Solution-state selectivity experiments

UV-Visible absorbance and fluorescence emission selectivity studies: A stock solution of compound **1** was prepared ([**1**] = 10 μM in acetonitrile). The UV-visible absorbance spectrum (between 200 and 800 nm) and steady-state fluorescence emission spectrum (λ_{ex} = 450 nm; scanned between 460 and 800 nm) of this solution were recorded. After that, a 100 nM aqueous solution of each analyte (analyte = H_2O_2, H_2O, I_2, and NaOCl) was added to the solution of compound **1** ($[analyte]_{final}$ = 10 nM), the solution was stirred manually, and the UV-visible absorbance and steady-state fluorescence emission spectra of each solution were re-measured. The UV-visible absorbance spectra were integrated between 375 and 700 nm, and the fluorescence emission spectra were integrated between 460 and 800 nm, using OriginPro software. The results reported herein represent an average of three independent trials.

Additional solution-state selectivity experiments were conducted by measuring the response of compound **1** to HCl and formaldehyde analytes: A stock solution of compound **1** was prepared ([**1**] = μM in acetonitrile). 3 mL of this solution was transferred to a cuvette, and the fluorescence emission spectrum of the solution was recorded (λ_{ex} = 450 nm; excitation and emission slit widths = 2.5 nm). After that, small amounts of an aqueous analyte solution were added (analyte = HCl, HCHO, or H_2O_2; $[analyte]_{final}$ = 30 mM), and the fluorescence emission spectrum of the solution was recorded every two minutes for one hour. The resulting data was analyzed using OriginPro software.

Colorimetric selectivity studies: A stock solution of compound **1** was prepared ([**1**] = 10 μM in acetonitrile). This solution was added to five vials (1 mL of the solution in each vial). A 100 μM aqueous solution of analyte (analyte = H_2O_2, H_2O, I_2, and NaCl; $[analyte]_{final}$ = 5 μM) was added to these vials. The samples were shaken manually, and allowed to sit at room temperature for five minutes. The vials were then photographed in both ambient lighting conditions and under 365 nm excitation, and the resulting images were subjected to quantitative colorimetric analysis (using ImageJ software). The results reported herein represent an average of three independent trials.

v. Real-world solution experiments

The response of compound **1** to hydrogen peroxide in Milli-Q water was compared to its response in untreated tap water. More specifically, we prepared a 10 μM solution of compound **1** in acetonitrile. 3.0 mL of that solution was transferred to a cuvette, and the steady-state fluorescence emission spectrum was recorded (λ_{ex} = 450 nm; scanned between 460 and 800 nm; excitation and emission slit widths = 2.5 nm). An aqueous hydrogen peroxide solution prepared in Milli-Q water was added to the acetonitrile solution of compound **1** ($[H_2O_2]_{final}$ = 30 mM), and the fluorescence emission spectrum of the solution was recorded every two minutes for one hour. The resulting data was analyzed using OriginPro software.

In a separate cuvette, 3.0 mL of the acetonitrile solution of compound **1** ([**1**] = 10 μM) was added. The fluorescence emission spectrum was recorded, under the same experimental parameters listed above. An aqueous solution of hydrogen peroxide in untreated tap water was added ($[H_2O_2]_{final}$ = 30 mM), and the fluorescence emission spectrum of the solution was recorded every two minutes for one hour. The resulting data was analyzed using OriginPro software.The pH and conductivity of both Milli-Q water and tap water were measured prior to the addition of H_2O_2. The results of these measurements are summarized in Table S13.

vi. Relative quantum yield calculations

The fluorescence spectra used to calculate the relative quantum yields were recorded using a Varian Cary Eclipse fluorescence spectrophotometer equipped with a 10 mm path length quartz cuvette. The excitation and emission slit widths were 2.5 nm each, and the scan rate was 120 nm/min. Quantum yields were calculated using the single point relative quantum yield method, according to Equation S3, below:[2]

$$\phi_{F(x)} = (n_x/n_s)^2 (A_s/A_x)(I_{f(x)}/I_{f(s)})\phi_{F(s)} \qquad \text{(Eq. S3)}$$

where ϕ_F represents the fluorescence quantum yield, A represents the absorbance value, I_f represents the integration of the fluorescence band, and n represents the solvent refractive index. The subscripts s and x refer to the standard sample and unknown sample, respectively. The standard

sample used in this work was a solution of 1,4-bis(5-phenyloxazol-2-yl)benzene (POPOP) in cyclohexane, which has a literature-reported quantum yield of 0.97.[3]

vii. Molar extinction coefficient calculations

To calculate the molar extinction coefficient of acetonitrile nitrile solutions of compound **2**, we used the Beer-Lambert equation, shown below:

$$A = \varepsilon \times c \times l \quad \text{(Eq. S4)}$$

where *A* represents the absorbance of the solution at a particular wavelength, ε represents the molar extinction coefficient, c represents the concentration (mol/L) and l represents the path length (cm). We used an 8 μM solution of compound **2** in acetonitrile and recorded the absorbance at 461 nm (A = 0.03966).

viii. Kinetics experiments

2.99 mL of a solution of compound **1** in acetonitrile ([**1**] = 10 μM) was transferred to a cuvette. The full UV-visible absorbance spectrum was recorded, as was the fluorescence emission spectrum (λ_{ex} = 450 nm, scanned between 460 and 800 nm). 10 μL of 30% hydrogen peroxide was added to the solution ($[H_2O_2]_{initial}$ = 8.8 M; $[H_2O_2]_{final}$ = 30 mM). The fluorescence emission spectrum was immediately re-recorded, and was subsequently re-recorded every two minutes for four hours. The same procedure was repeated a second time with water as the analyte, with the water introduced as an acetonitrile solution ($[H_2O]_{initial}$ = 8.8 M; $[H_2O]_{final}$ = 30 mM). The fluorescence emission spectrum of compound **1** was recorded immediately following the addition of water, and at two-minute intervals for four hours. The same procedure was repeated a third time using an excess of water ($[H_2O]_{final}$ = 129 mM, the amount of water present in the H_2O_2 sample). The fluorescence emission spectrum of compound **1** was recorded immediately following the addition of water, and at two-minute intervals for four hours.

c. Filter paper-based experiments

i. Fabrication of compound **1** – functionalized filter papers

Compound **1** was adsorbed onto Whatman #1 filter papers by submerging the filter papers overnight at room temperature in a solution of compound **1** in acetone ([**1**] = 50 μM). Following overnight submersion, the papers were removed from the solution with tweezers, and were allowed to dry in an open-air environment.

ii. Evaluation of colorimetric response of compound **1** – functionalized filter papers to hydrogen peroxide in solution

The as-prepared papers were exposed to 10 μL of hydrogen peroxide in acetonitrile of varying concentrations ($[H_2O_2]$ = 0, 5, 10, 15, 20, 25, 30, 35, 40, 45, and 50 mM), which were added via pipette. The papers were allowed to rest under ambient conditions for five minutes, and then were photographed under ambient light and under 365 nm excitation (using a hand-held TLC lamp). Colorimetric analysis of the resulting photographs was conducted using ImageJ software. The results reported herein represent an average of three independent trials.

iii. Evaluation of colorimetric response of compound **1** – functionalized filter papers to water in solution

The same procedure was repeated using solutions of water in acetonitrile of varying concentrations ($[H_2O]$ = 0, 5, 10, 15, 20, 25, 30, 35, 40, 45, and 50 mM). 10 μL of each solution was added to the compound **1** – functionalized filter papers, followed by allowing the papers to rest under ambient conditions for five minutes. The papers were then photographed under ambient light and under 365 nm excitation (using a hand-held TLC lamp). Colorimetric analysis of the resulting photographs was conducted using ImageJ software. The results reported herein represent an average of three independent trials.

iv. Evaluation of colorimetric response of compound **1** – functionalized filter papers to vapor-phase hydrogen peroxide

Circular Whatman #1 filter papers with a diameter of 6 mm were coated with a solution of compound **1**, by submerging the filter papers in a solution of compound **1** ([**1**] = 50 μM in acetone) overnight at room temperature. The filter papers were then removed using tweezers and allowed to dry under ambient conditions. In the interim, a 2 mL glass vial was saturated with hydrogen peroxide vapors, by adding 1 mL of a solution of 30% H_2O_2 (w/v) to the vial, diluted to achieve a range of final concentrations ($[H_2O_2]_{final}$ = 0, 20, 40, 60, 80, and 100 mM), and allowing the vials to remain sealed for one hour. After one hour, a functionalized filter paper dot was affixed to the inside of the cap of the H_2O_2-saturated vial using double-sided tape, and the vial was re-sealed for ten minutes to allow exposure of the compound **1** - functionalized dot to the H_2O_2 vapor. After ten minutes, the functionalized dot was removed from the cap, and photographed under excitation by a long-wave, hand-held TLC lamp (λ_{ex} = 365 nm). Colorimetric analysis of the resulting photographs was conducted using ImageJ software. The results reported herein represent an average of three independent trials. As a control experiment, compound **1** – functionalized dots were also exposed to water vapor, by saturating a 2 mL vial with 1 mL of deionized water prior to introduction of the functionalized dot.

v. Vapor-phase selectivity experiments

Circular Whatman #1 filter papers were coated with a solution of compound **1**, by submerging the filter papers in a solution of compound **1** ([**1**] = 50 μM in acetone) overnight at room temperature. The filter papers were then removed using tweezers and allowed to dry under ambient conditions. In the interim, 2-mL glass vials were saturated with vapors of various analytes, by adding 1 mL of an aqueous solution of each analyte to a vial and allowing the sealed vial to equilibrate at room temperature for one hour (analyte = H_2O_2, H_2O, I_2, NaOCl, HCl, HCHO; [analyte] = 10 mM in water). After one hour, a functionalized filter paper dot was affixed to the inside of the cap of the analyte-saturated vial using double-sided tape, and the vial was re-sealed for ten minutes to allow exposure of the compound **1** - functionalized dot to the analyte vapor. After ten minutes, the functionalized dot was removed from the cap, and photographed under excitation by a long-wave, hand-held TLC lamp (λ_{ex} = 365 nm). Colorimetric analysis of the resulting photographs was conducted using ImageJ software. The results reported herein represent an average of three independent trials. As a control experiment, compound **1** – functionalized dots were also photographed in the absence of any analyte exposure, and the resulting photographs were subject to similar colorimetric analysis.

vi. Calculations of vapor phase concentration

Calculations of the concentration of hydrogen peroxide in the vapor phase were conducted as follows: A 10 mM aqueous solution of hydrogen peroxide has an equilibrium vapor pressure of 1.20E-7 atm (using Henry's law constant of $K_H = 8.33 \pm 0.38 \times 10^4$ M-atm^{-1} at 25 °C).[4]

- 1.20E-7 atm = 9.12E-5 mm Hg
- ppm = (9.12E-5 mm Hg)/ (760 mm Hg) x 1E6 = 0.12 ppm

vii. Assessment of the reusability of compound **1** – functionalized papers

Compound **1** – functionalized filter papers were fabricated: Whatman #1 filter paper was cut into circles with a diameter of 6 mm, and soaked overnight in a solution of compound **1** in acetone ([**1**] = 50 μM). The dots were removed from the solution using tweezers, dried under ambient conditions, and photographed under 365 nm excitation (using a hand-held TLC lamp).

Compound **1** – functionalized papers were reacted with H_2O_2: Filter papers functionalized with compound **1** were exposed to 10 μL of a 50 mM H_2O_2 solution (made from dilution of a 30% H_2O_2 solution). The papers were allowed to dry at room temperature, and were photographed under 365 nm excitation (using a hand-held TLC lamp).

The following procedure was executed to attempt to regenerate the functionalized papers: The filter papers were dried at 80 °C for 10 minutes, followed by the addition of 10 μL of boric acid ([boric acid] = 50 μM) via micropipette. 10 μL of pinacol was immediately added to the dots via micropipette, and the dots were allowed to dry under ambient conditions for 30 minutes. The resulting dots were then photographed under 365 nm excitation (using a hand-held TLC lamp), and the photograph was compared with the photograph of the original dots prior to H_2O_2 exposure.

d. *^{1}H NMR titration experiments*

2.5 mg of compound **1** were dissolved in 450 μL of DMSO-d_6, and the ^{1}H NMR spectrum was recorded. We then added 20 μL of H_2O_2 (30% (w/v), 8.8 M), vortexed the NMR tube, and re-recorded the ^{1}H NMR spectrum. We continued to add H_2O_2 solution (30% (w/v), 8.8 M) in increments of 20 μL, up to a total addition volume of 160 μL, re-recording the ^{1}H NMR spectrum after each addition.

III. SUMMARY TABLES

a. *Solution-state experiments*

i. Water vs. hydrogen peroxide response comparison

Table S1. Summary of the UV-visible absorbance data of solutions of compound **1**, as a function of increasing concentrations of hydrogen peroxide[a]

$[H_2O_2]$ (M)	Normalized integration[b]	I_{457nm}[c]
0	0.97 ± 0.03	0.23 ± 0.01
0.087	0.95 ± 0.03	0.23 ± 0.00
0.17	0.93 ± 0.02	0.22 ± 0.00
0.26	0.91 ± 0.02	0.21 ± 0.01
0.34	0.90 ± 0.03	0.21 ± 0.01
0.42	0.88 ± 0.02	0.20 ± 0.01
0.50	0.86 ± 0.03	0.19 ± 0.01
0.58	0.84 ± 0.03	0.18 ± 0.01
0.65	0.82 ± 0.03	0.18 ± 0.01

[a] [**1**] = 10 μM; all results represent the average of three independent trials

[b] UV-visible absorbance spectra were integrated between 370 and 600 nm, using OriginPro software

[c] I_{457nm} represents the absorption intensity of the solution at 457 nm

Table S2. Summary of the UV-visible absorbance data of solutions of compound **1**, as a function of increasing concentrations of water[a]

$[H_2O]$ (M)	Normalized integration[b]	I_{457nm}[c]
0	0.99 ± 0.02	0.24 ± 0.01
0.55	0.98 ± 0.01	0.23 ± 0.00
1.09	0.96 ± 0.01	0.23 ± 0.00
1.62	0.96 ± 0.00	0.23 ± 0.00
2.13	0.94 ± 0.00	0.22 ± 0.00
2.64	0.93 ± 0.00	0.22 ± 0.00
3.14	0.92 ± 0.00	0.22 ± 0.00
3.63	0.92 ± 0.01	0.22 ± 0.00
4.11	0.91 ± 0.00	0.21 ± 0.00

[a] [**1**] = 10 μM; all results represent the average of three independent trials

[b] UV-visible absorbance spectra were integrated between 370 and 600 nm, using OriginPro software

[c] I_{457nm} represents the absorption intensity of the solution at 457 nm

Table S3. Summary of the fluorescence emission data of solutions of compound **1**, as a function of increasing concentrations of hydrogen peroxide[a]

$[H_2O_2]$ (M)	Normalized integration[b]	I_{534nm}[c]
0	0.96 ± 0.01	304.8 ± 2.6
0.087	0.72 ± 0.01	220.3 ± 2.6
0.17	0.55 ± 0.00	161.7 ± 0.1
0.26	0.38 ± 0.01	108.2 ± 1.8
0.34	0.26 ± 0.01	69.1 ± 3.5
0.42	0.17 ± 0.01	43.1 ± 1.5
0.50	0.11 ± 0.01	25.1 ± 3.3
0.58	0.05 ± 0.01	10.0 ± 2.6
0.65	0.03 ± 0.01	3.6 ± 1.9

[a] [**1**] = 10 μM; $\lambda_{excitation}$ = 450 nm; all results represent the average of three independent trials
[b] Fluorescence emission spectra were integrated between 460 and 800 nm, using OriginPro software
[c] I_{534nm} represents the emission intensity of the solution at 534 nm

Table S4. Summary of the fluorescence emission data of solutions of compound **1**, as a function of increasing concentrations of water[a]

$[H_2O]$ (M)	Normalized integration[b]	I_{534nm}[c]
0	0.97 ± 0.04	315.2 ± 9.4
0.55	0.90 ± 0.04	289.5 ± 12.0
1.09	0.85 ± 0.04	269.7 ± 11.2
1.62	0.80 ± 0.04	252.3 ± 17.0
2.13	0.76 ± 0.05	234.7 ± 17.0
2.64	0.72 ± 0.05	221.0 ± 17.6
3.14	0.69 ± 0.05	206.5 ± 18.5
3.63	0.65 ± 0.05	193.8 ± 18.5
4.11	0.63 ± 0.05	184.3 ± 18.6

[a] [**1**] = 10 μM; $\lambda_{excitation}$ = 450 nm; all results represent the average of three independent trials
[b] Fluorescence emission spectra were integrated between 460 and 800 nm, using OriginPro software
[c] I_{534nm} represents the emission intensity of the solution at 534 nm

ii. Limit of detection experiments

Table S5. Limits of detection and quantification of hydrogen peroxide in solution, using changes to the photophysical properties of compound **1** upon exposure to varying analyte concentrations[a]

Output value	Linear Equation	R^2 value	Limit of Detection (nM)	Limit of Quantification (nM)
Integrated UV-visible absorbance spectra (370-600 nm)	y = -2134.9x + 1083.8	0.9999	0.028 ± 0.002	0.096 ± 0.005
Intensity of absorbance (at 455 nm)	y = -0.4644x + 0.2375	0.9999	0.019 ± 0.001	0.064 ± 0.002
Integrated fluorescence emission spectra (460-800 nm)	y = -1E6x + 743950	0.9989	0.0079 ± 0.0002	0.0315 ± 0.0002
Intensity of fluorescence emission (at 534 nm)	y = -462.69x + 325.46	0.9991	0.0091 ± 0.0001	0.0357 ± 0.0002

[a] [**1**] = 10 μM in acetonitrile; [H_2O_2] = 0, 0.005, 0.01, 0.05, 0.1, 0.15 nM

Table S6. Selected examples of literature-reported limits of detection for hydrogen peroxide sensors

Sensing compound	Detection method	Limit of detection (LOD)	Reference
Platinum/ porous graphene	Electrochemical	0.50 μM	*5*
Prussian blue nanoparticles	Colorimetric	0.03 μM	*6*
Tetraphenylene derivative	Fluorometric (via aggregation-induced emission)	10 nM	*7*
Silver/gold nanomaterials	UV-visible extinction spectroscopy	1.11 μM	*8*
Ni-Fe nanocubes	Electrochemical	0.291 μM	*9*
Coumarin-naphthalimide hybrid	Fluorometric	0.28 μM	*10*
Polyoxometalate	Fluorometric	3.8 nM	*11*
Boronic acid	Fluorometric	1.8 nM	*12*

iii. Solution-state colorimetric analysis

H_2O_2 analyte

Ambient lighting:

Table S7. Quantitative colorimetric values of solutions of compound **1** as a function of exposure to varying concentrations of hydrogen peroxide, viewed under ambient lighting

[H_2O_2] (mM)	Red	Green	Blue	(R+G+B)/ 3	0.299R + 0.587G + 0.114B
0	183.8 ± 5.8	185.2 ± 5.6	102.3 ± 3.7	157.1 ± 5.0	175.3 ± 5.4
60	175.3 ± 9.1	170.7 ± 10.3	108.0 ± 4.9	151.3 ± 8.1	164.9 ± 9.3
120	178.9 ± 13.8	172.6 ± 13.3	117.7 ± 10.8	156.4 ± 11.9	168.2 ± 12.8
180	179.4 ± 8.2	172.8 ± 8.3	126.1 ± 4.7	159.4 ± 6.8	169.4 ± 7.7
240	184.3 ± 7.8	178.2 ± 7.6	141.3 ± 5.3	168.0 ± 6.7	175.8 ± 7.3
300	213.8 ± 1.5	207.4 ± 1.1	178.1 ± 1.9	199.9 ± 1.5	206.0 ± 1.4

[a] [**1**] = 10 μM in acetonitrile; all results represent the average of three independent trials

365 nm excitation:

Table S8. Quantitative colorimetric values of solutions of compound **1** as a function of exposure to varying concentrations of hydrogen peroxide, viewed under 365 nm excitation[a]

[H_2O_2] (mM)	Red	Green	Blue	(R+G+B)/3	0.299R + 0.587G + 0.114B
0	163.6 ± 3.8	246.6 ± 9.4	1.5 ± 0.0	137.2 ± 2.2	193.8 ± 4.6
60	191.9 ± 4.5	241.7 ± 7.3	1.3 ± 0.2	145.0 ± 3.8	199.4 ± 5.4
120	204.7 ± 14.1	200.8 ± 34.8	17.2 ± 14.0	140.9 ± 9.7	181.0 ± 19.8
180	193.4 ± 19.9	161.6 ± 27.2	30.2 ± 16.3	128.4 ± 10.3	156.2 ± 18.3
240	150.5 ± 21.3	109.9 ± 30.8	30.7 ± 8.9	97.0 ±17.4	113.0 ± 24.0
300	91.6 ± 5.7	59.3 ± 2.8	28.0 ± 2.7	59.6 ± 1.7	65.4 ± 2.7

[a] [**1**] = 10 μM in acetonitrile; all results represent the average of three independent trials

H_2O analyte

Ambient lighting:

Table S9. Quantitative colorimetric values of solutions of compound **1** as a function of exposure to varying concentrations of water, viewed under ambient lighting[a]

[H_2O] (mM)	Red	Green	Blue	(R+G+B)/3	0.299R + 0.587G + 0.114B
0	191.0 ± 12.2	190.4 ± 12.0	104.9 ± 9.1	162.1 ± 11.0	180.9 ± 11.7
60	182.8 ± 9.2	183.9 ± 8.7	105.8 ± 7.8	157.4 ± 8.6	174.7 ± 8.8

120	186.0 ± 9.9	186.9 ± 9.2	114.1 ± 7.2	162.3 ± 8.7	178.4 ± 9.2
180	186.1 ± 11.6	186.2 ± 11.0	119.7 ± 9.1	164.1 ± 10.6	178.6 ± 11.0
240	193.5 ± 6.7	191.9 ± 6.5	136.4 ± 5.8	174.1 ± 6.4	186.1 ± 6.5
300	224.2 ± 2.8	221.2 ± 2.3	174.5 ± 1.3	206.7 ± 1.9	216.9 ± 2.3

[a] [**1**] = 10 μM in acetonitrile; all results represent the average of three independent trials

365 nm excitation:

Table S10. Quantitative colorimetric values of solutions of compound **1** as a function of exposure to varying concentrations of water, viewed under 365 nm excitation[a]

[H_2O_2] (mM)	Red	Green	Blue	(R+G+B)/ 3	0.299R + 0.587G + 0.114B
0	114.5 ± 6.5	175.5 ± 4.3	1.4 ± 0.1	97.1 ± 3.3	137.4 ± 4.2
60	138.9 ± 7.2	213.6 ± 7.5	1.4 ± 0.2	117.9 ± 4.6	167.0 ± 6.3
120	145.8 ± 7.1	222.6 ± 4.5	1.7 ± 0.3	123.4 ± 3.8	174.4 ± 4.6
180	142.4 ± 6.8	214.0 ± 2.8	1.6 ± 0.3	119.4 ± 3.2	168.4 ± 3.6
240	124.7 ± 5.6	186.2 ± 1.9	1.5 ± 0.3	104.2 ± 1.6	146.7 ± 1.3
300	96.7 ± 2.1	144.0 ± 5.6	4.2 ± 1.3	81.6 ± 1.5	113.8 ± 3.1

[a] [**1**] = 10 μM in acetonitrile; all results represent the average of three independent trials

iv. Solution-state selectivity experiments

Table S11. Normalized integration values of UV-visible absorbance and fluorescence emission spectra of solutions of compound **1** ([**1**] = 10 μM in acetonitrile) after exposure to various analytes[a]

Analyte	Integrated absorbance	Integrated fluorescence
None	1.00 ± 0.000	1.00 ± 0.0001
NaOCl	0.87 ± 0.002	0.94 ± 0.0004
I_2	0.87 ± 0.002	0.94 ± 0.0003
H_2O_2	0.86 ± 0.002	0.94 ± 0.0001
H_2O	0.85 ± 0.002	0.99 ± 0.0004

[a] Analyte exposure was accomplished through the addition of small amounts of a 100 nM aqueous solution of each analyte ($[analyte]_{final}$ = 10 nM). UV-visible absorbance spectra were integrated between 375 and 700 nm; fluorescence emission spectra were integrated between 460 and 800 nm. All results represent an average of three independent trials.

Table S12. Quantitative colorimetric values of solutions of compound **1** after exposure to various analytes, photographed under ambient lighting and under 365 nm excitation[a]

Conditions	Analyte	Red	Green	Blue	(R+G+B)/3	0.299R + 0.587G + 0.114B
λ_{ex} = 365 nm	blank	112.0 ± 3.9	176.0 ± 8.9	1.2 ± 0.1	96.4 ± 3.3	136.9 ± 5.5
	H_2O_2	124.2 ± 2.9	168.4 ± 8.3	1.3 ± 0.1	98.0 ± 3.7	136.1 ± 5.7
	H_2O	120.4 ± 4.6	191.7 ± 7.1	1.5 ± 0.7	104.5 ± 2.9	148.7 ± 4.3
	I_2	131.9 ± 4.1	178.8 ± 5.2	1.6 ± 0.4	104.1 ± 2.4	144.5 ± 3.6
	NaOCl	9.5 ± 4.3	16.0 ± 5.0	15.1 ± 4.6	13.5 ± 4.6	14.0 ± 4.7
Ambient lighting	blank	176.9 ± 5.6	178.7 ± 5.7	106.0 ± 4.1	153.7 ± 5.2	169.9 ± 5.5
	H_2O_2	172.0 ± 4.6	171.2 ± 4.7	108.5 ± 0.1	150.5 ± 3.3	164.4 ± 4.2
	H_2O	174.0 ± 4.5	176.1 ± 4.3	110.6 ± 4.2	153.6 ± 4.2	168.0 ± 4.2
	I_2	177.0 ± 4.6	176.1 ± 4.5	114.4 ± 2.4	155.8 ± 3.9	169.4 ± 4.3
	NaOCl	195.6 ± 2.6	196.2 ± 2.6	184.5 ± 4.9	192.1 ± 3.3	194.7 ± 2.8

[a] [**1**] = 10 μM; $[analyte]_{final}$ = 5 μM; UV excitation photographs were taken with 365 nm excitation using a hand-held TLC lamp; all photographs were analyzed using ImageJ software and the results represent an average of three independent trials

Table S13. Percent fluorescence decrease of solutions of compound **1** after exposure to 30 mM hydrochloric acid (HCl), formaldehyde (HCHO), or hydrogen peroxide (H_2O_2) in Milli-Q water[a]

Time (min)	% decrease after HCl addition	% decrease after HCHO addition	% decrease after H_2O_2 addition
0	0.0 %	0.0 %	0.0 %
10	23.6 %	2.4 %	16.8 %
20	24.0 %	2.5 %	19.9 %
30	24.4 %	2.4 %	22.3 %
40	24.7 %	2.4 %	24.1 %
50	25.1 %	2.4 %	25.8 %
60	25.4 %	2.5 %	27.1 %

[a] [**1**] = 10 μM in acetonitrile; [analyte] = 30 mM; Percent decrease = $(Fl_{initial}\text{-}Fl_{final})/Fl_{initial}$ * 100%, where $Fl_{initial}$ represents the integrated fluorescence emission prior to the addition of analyte, and Fl_{final} represents the integrated fluorescence emission after the addition of analyte

v. Real-world solution experiments

Table S14. Summary of the pH and conductivity measurements of purified Milli-Q water compared to untreated tap water

Aqueous system	pH (without H_2O_2)	Conductivity (without H_2O_2; measured as μS/cm)
Milli-Q water	6.9	4.24
Untreated tap water	7.6	905

Table S15. Percent fluorescence decrease of solutions of compound **1** after exposure to 30 mM hydrogen peroxide in purified Milli-Q water and in untreated tap water[a]

Time (min)	Percent decrease in Milli-Q water	Percent decrease in untreated tap water
0	0.0 %	0.0 %
10	16.8 %	20.1 %
20	19.9 %	25.9 %
30	22.3 %	31.0 %
40	24.1 %	35.6 %
50	25.8 %	39.8 %
60	27.1 %	42.8 %

[a] [**1**] = 10 μM in acetonitrile; [H_2O_2] = 30 mM; Percent decrease = ($Fl_{initial}$-Fl_{final})/$Fl_{initial}$ * 100%, where $Fl_{initial}$ represents the integrated fluorescence emission prior to the addition of hydrogen peroxide, and Fl_{final} represents the integrated fluorescence emission after the addition of hydrogen peroxide

vi. Relative quantum yield experimental results

Table S16. Summary of experimental data about cyclohexane solutions of the standard sample used to calculate the relative quantum yield of compound **2**

Experimental parameter	**Experimentally-obtained value**
Refractive index of acetonitrile (n_x)	1.3441
Refractive index of cyclohexane (n_s)	1.4266
Absorbance value of standard sample (A_s)	0.03235
Integration value of fluorescence band for standard sample ($I_{F(s)}$)	6888.96
Fluorescence quantum yield for standard sample ($\phi_{F(s)}$)	0.97

Table S17. Summary of experimental data about acetonitrile solutions of compound **2** used to calculate the relative quantum yield of compound **2**

[**2**] (μM)	Absorbance Value (A_x)	Integration value ($I_{F(x)}$)	Quantum Yield ($\phi_{F(x)}$)
8	0.03966	411.74	0.042
7	0.03392	361.31	0.043
6	0.02921	318.36	0.044

Average relative quantum yield = 0.043

vii. Molar extinction coefficient experimental results

Table S18. Summary of experimental data used to calculate the molar extinction coefficient of compound **2**

Experimental parameter	**Experimentally-obtained value**
Absorbance of compound **2** in acetonitrile (A)	0.03966
Concentration of compound **2** (c)	8×10^{-6} mol/ L
Path length	1 cm
Molar Extinction Coefficient	**4.957×10^3 L M^{-1} cm^{-1}**

viii. Kinetics experiments

Table S19. Summary of the normalized integrated fluorescence emission of solutions of compound **1** after exposure to hydrogen peroxide (30 mM), water (30 mM), and water (129 mM), as a function of time[a]

Time (min)	H_2O_2 (30 mM)	H_2O (30 mM)	H_2O (129 mM)
0	1.00	0.99	0.97
20	0.79	0.98	0.95
40	0.68	0.98	0.95
60	0.59	0.98	0.95
80	0.52	0.98	0.95
100	0.46	0.98	0.95
120	0.41	0.98	0.95
140	0.37	0.98	0.95
160	0.34	0.98	0.95
180	0.31	0.98	0.95
200	0.29	0.98	0.95
220	0.27	0.98	0.95

[a] [**1**] = 10 μM in acetonitrile; λ_{ex} = 450 nm; emission recorded 460-800 nm

b. Filter paper-based experiments

i. Analyte detection in solution using compound **1** – functionalized papers

H_2O_2 analyte

Table S20. Quantitative colorimetric values of Whatman #1 filter papers onto which compound **1** was adsorbed, after exposure to varying concentrations of hydrogen peroxide, viewed under 365 nm excitation[a]

[H_2O_2] (mM)	Red	Green	Blue	(R+G+B)/3	0.299R + 0.587G + 0.114B
0	211.9 ± 10.4	173.3 ± 14.5	80.0 ± 12.4	155.1 ± 12.0	174.2 ± 12.8
5	179.1 ± 5.2	134.5 ± 10.6	93.8 ± 14.2	135.9 ± 8.1	143.2 ± 7.6
10	176.3 ± 11.7	130.8 ± 12.7	98.2 ± 8.4	135.1 ± 8.9	140.7 ± 10.8
15	164.2 ± 7.6	122.9 ± 10.7	105.8 ± 8.3	131.0 ± 7.9	133.3 ± 8.8
20	157.4 ± 6.5	118.2 ± 5.3	106.0 ± 12.6	127.2 ± 4.4	128.5 ± 3.7
25	140.9 ± 8.7	102.3 ± 4.4	100.0 ± 9.4	114.4 ± 3.7	113.6 ± 3.4
30	138.0 ± 12.5	98.5 ± 8.2	94.9 ± 8.1	110.5 ± 8.1	109.9 ± 8.6
35	149.9 ± 12.7	104.5 ± 9.2	99.3 ± 8.1	117.9 ± 9.8	117.5 ± 10.0
40	153.5 ± 17.3	109.3 ± 12.9	103.3 ± 10.9	122.0 ± 11.8	121.9 ± 13.0
45	135.4 ± 5.1	97.8 ± 2.5	102.4 ± 11.6	111.9 ± 3.4	109.6 ± 1.7
50	133.3 ± 13.3	95.7 ± 8.9	100.6 ± 3.2	109.9 ± 7.6	107.5 ± 9.3

[a] Functionalized filter papers were formed by submerging Whatman #1 filter paper in acetone solutions of compound **1** (see experimental procedures for more details); all results represent the average of three independent trials

H_2O analyte

Table S21. Quantitative colorimetric values of Whatman #1 filter papers onto which compound **1** was adsorbed, after exposure to varying concentrations of water, viewed under 365 nm excitation[a]

[H_2O] (mM)	Red	Green	Blue	(R+G+B)/3	0.299R + 0.587G + 0.114B
0	189.8 ± 6.9	155.2 ± 5.8	68.5 ± 11.1	137.8 ± 7.0	155.7 ± 6.3
5	171.9 ± 13.4	148.3 ± 12.8	57.7 ± 10.9	126.0 ± 12.2	145.0 ± 12.7
10	170.4 ± 6.1	147.7 ± 7.3	69.7 ± 11.8	129.3 ± 8.0	145.6 ± 7.3
15	160.4 ± 12.7	138.0 ± 12.0	70.0 ± 7.6	122.8 ± 8.6	136.9 ± 10.9
20	169.0 ± 9.7	145.1 ± 9.9	73.6 ± 11.9	129.2 ± 10.5	144.1 ± 10.1
25	146.6 ± 13.0	128.2 ± 13.0	71.1 ± 11.6	115.4 ± 12.5	127.2 ± 12.8
30	154.2 ± 18.4	132.2 ± 16.8	66.2 ± 13.9	117.5 ± 16.3	131.2 ± 16.9
35	161.4 ± 4.3	137.6 ± 4.9	70.8 ± 11.2	123.2 ± 6.6	137.1 ± 5.3
40	164.8 ± 5.0	139.3 ± 5.4	67.9 ± 7.2	124.0 ± 5.8	138.8 ± 5.4
45	163.1 ± 11.0	139.8 ± 10.9	67.8 ± 10.7	123.5 ± 10.7	138.5 ± 10.8
50	151.5 ± 6.1	129.8 ± 3.4	69.2 ± 9.0	116.8 ± 0.5	129.3 ± 2.8

[a] Functionalized filter papers were formed by submerging Whatman #1 filter paper in acetone solutions of compound **1** (see experimental procedures for more details); all results represent the average of three independent trials

ii. Vapor-phase analyte detection using compound **1** – functionalized papers

Table S22. Summary of quantitative colorimetric data of compound **1** – functionalized papers after exposure to vapor-phase H_2O_2[a]

[H_2O_2] (mM)	Red	Green	Blue	(R+G+B)/3	0.299R+0.587G+0.114B
0	234.5 ± 0.4	161.2 ± 0.6	53.8 ± 0.5	149.9 ± 0.5	170.9 ± 0.5
20	203.8 ± 13.3	136.0 ± 2.2	27.6 ± 24.7	122.5 ± 24.7	143.9 ± 24.7
40	190.5 ± 24.2	129.8 ± 13.1	28.1 ± 27.2	116.1 ± 27.2	136.4 ± 27.2
60	184.8 ± 20.5	118.8 ± 8.6	31.6 ± 18.4	111.7 ± 18.4	128.6 ± 18.4
80	181.5 ± 20.9	117.5 ± 7.7	32.1 ± 23.1	110.4 ± 23.1	126.9 ± 23.1
100	160.5 ± 21.1	97.4 ± 11.1	40.9 ± 20.6	99.6 ± 20.6	109.8 ± 20.6
water	199.9 ± 13.0	133.1 ± 5.7	24.0 ± 23.3	119.0 ± 23.3	140.7 ± 23.3

[a] Quantitative colorimetric values were calculated using ImageJ software, based on the images taken of the compound **1** – functionalized dots after exposure to vapor-phase H_2O_2 (or water). All results represent the average of three independent trials.

iii. Vapor-phase selectivity experiments using compound **1** – functionalized papers

Table S23. Summary of quantitative colorimetric data of compound **1** – functionalized papers after exposure to various vapor-phase analytes[a]

Analyte	Red	Green	Blue	(R+G+B)/3	0.299R+0.587G+0.114B
blank	229.5 ± 17.1	210.4 ± 11.5	31.6 ± 16.6	157.2 ± 4.1	195.7 ± 9.9
H_2O	216.9 ± 23.9	172.4 ± 8.2	36.2 ± 18.9	141.7 ± 5.0	170.2 ± 9.9
H_2O_2	162.0 ± 34.2	116.3 ± 15.3	57.0 ± 33.6	111.8 ± 5.3	123.2 ± 15.3
I_2	99.1 ± 19.2	86.0 ± 9.6	10.5 ± 4.3	65.2 ± 8.4	81.4 ± 10.5
NaOCl	204.7 ± 12.4	160.9 ± 7.8	39.9 ± 21.3	135.2 ± 4.1	160.2 ± 4.9

[a] Quantitative colorimetric values were calculated using ImageJ software, based on the images taken of the compound **1** – functionalized dots after exposure to vapor-phase analytes, photographed under 365 nm excitation. All results represent the average of three independent trials.

iv. Assessment of reusability experiments using compound 1 – functionalized papers

Table S24. Summary of the colorimetric values of compound **1** – functionalized filter papers photographed under 365 nm excitation: before analyte exposure, after exposure to a 50 mM H_2O_2 solution, and after treatment with boric acid and pinacol[a]

Colorimetric value	Before analyte exposure	After H_2O_2 exposure	After treatment with boric acid and pinacol
Red	173.6 ± 1.5	61.7 ± 3.3	66.1 ± 4.3
Green	152.0 ± 2.2	35.0 ± 2.2	25.9 ± 2.6
Blue	42.7 ± 3.3	62.4 ± 1.5	37.8 ± 1.0
(R+G+B)/3	122.7 ± 1.5	53.0 ± 2.2	43.3 ± 2.5
0.299R+0.587G+0.114B	146.0 ± 1.7	46.1 ± 2.4	39.3 ± 2.9

[a] Colorimetric values were obtained using ImageJ software; all results represent an average of three independent trials

IV. SUMMARY FIGURES

a. *Synthesis figures*

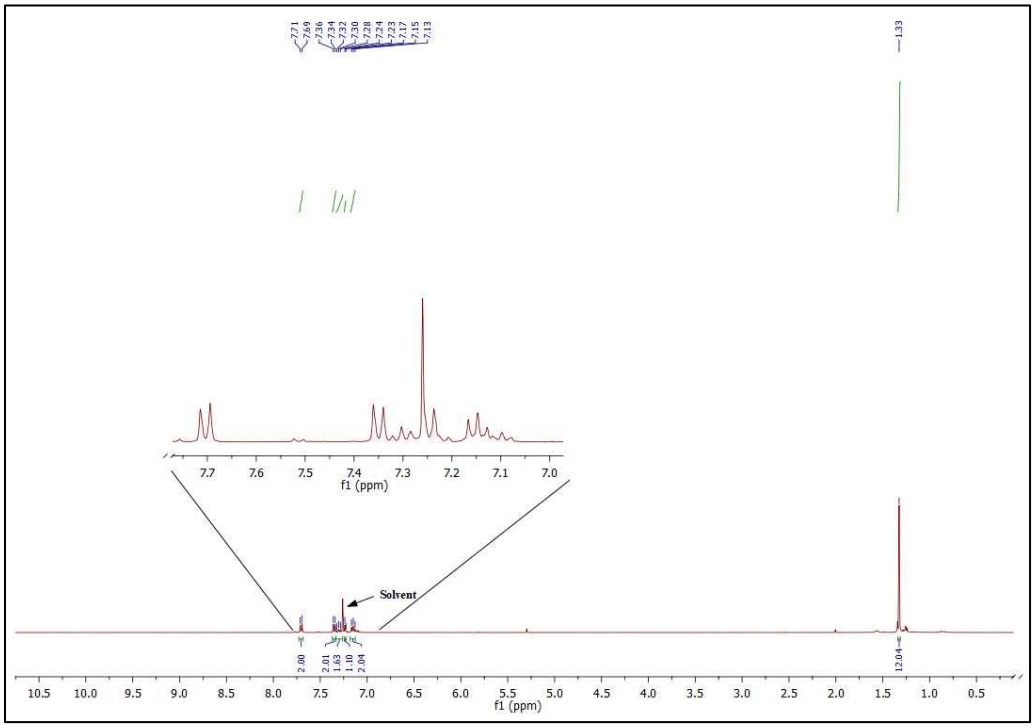

Figure S3. ^{1}H NMR spectrum of compound **1** in $CDCl_3$

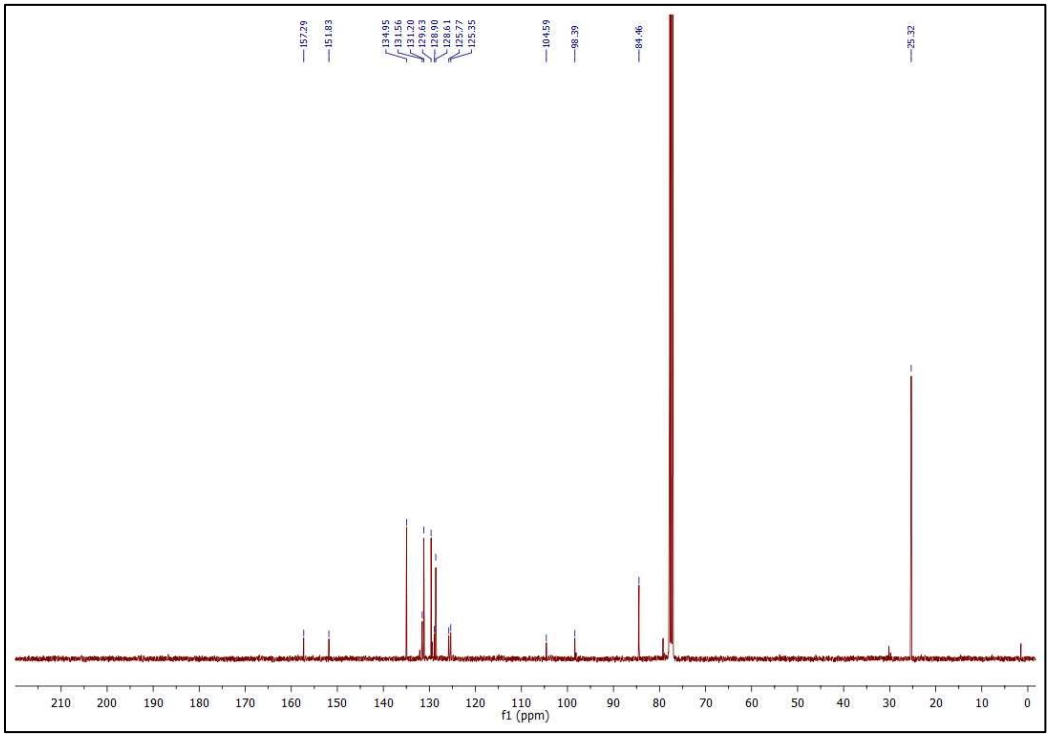

Figure S4. ^{13}C NMR spectrum of compound **1** in $CDCl_3$

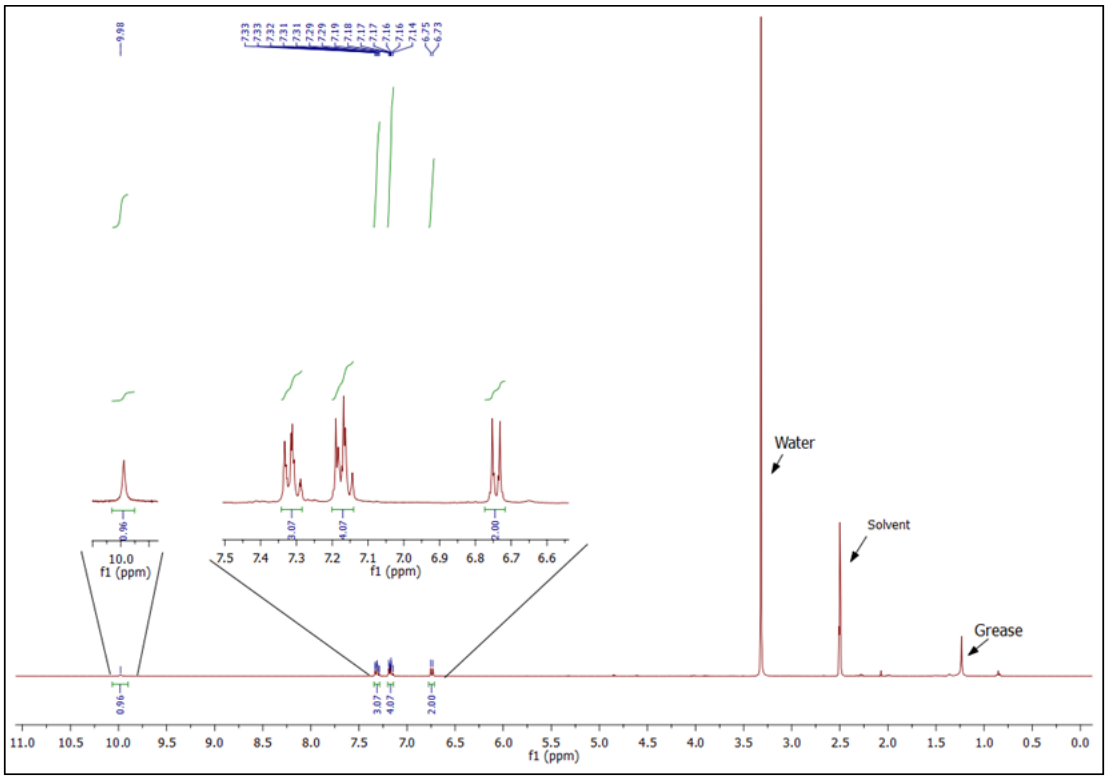

Figure S5. ^{1}H NMR spectrum of compound **2** in DMSO-d_6

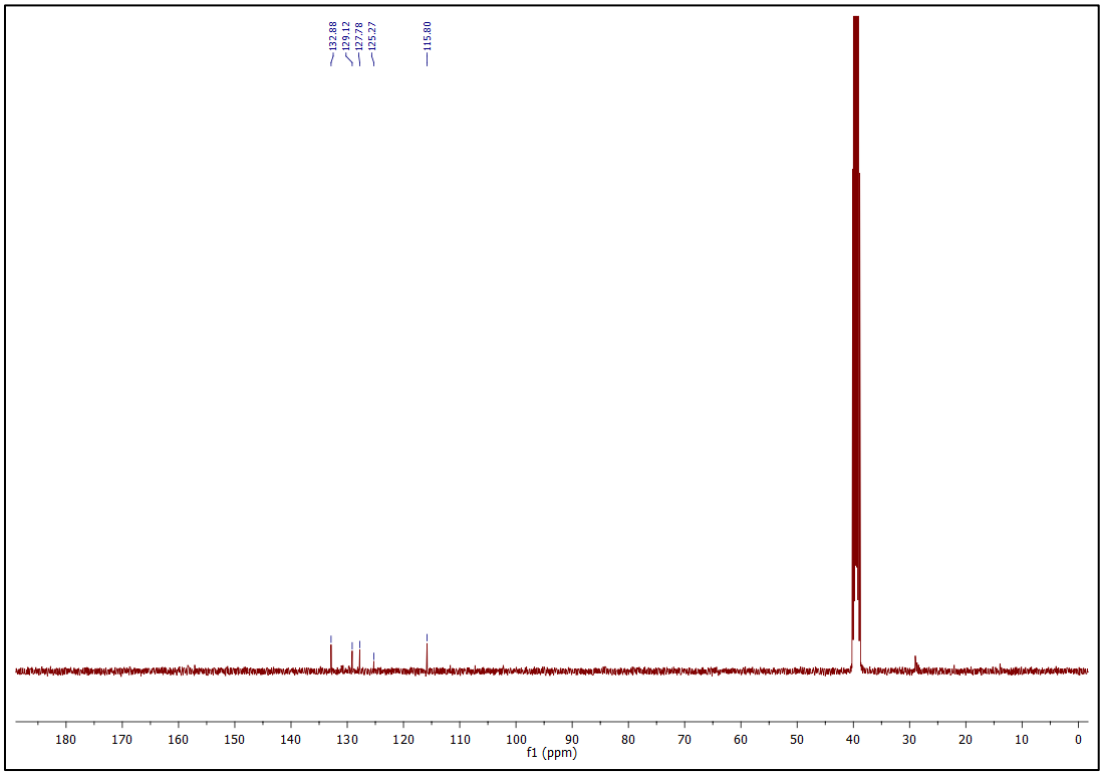

Figure S6. ^{13}C NMR spectrum of compound **2** in DMSO-d_6

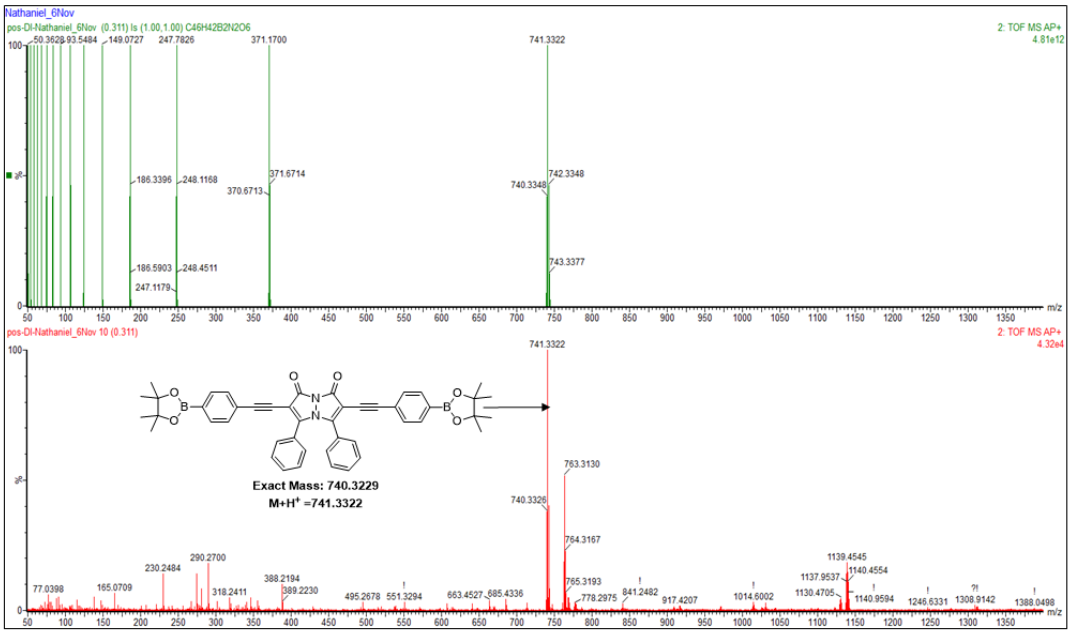

Figure S7. High resolution mass spectrum (HRMS) of compound **1** (top: computationally predicted spectrum; bottom: experimentally-obtained spectrum)

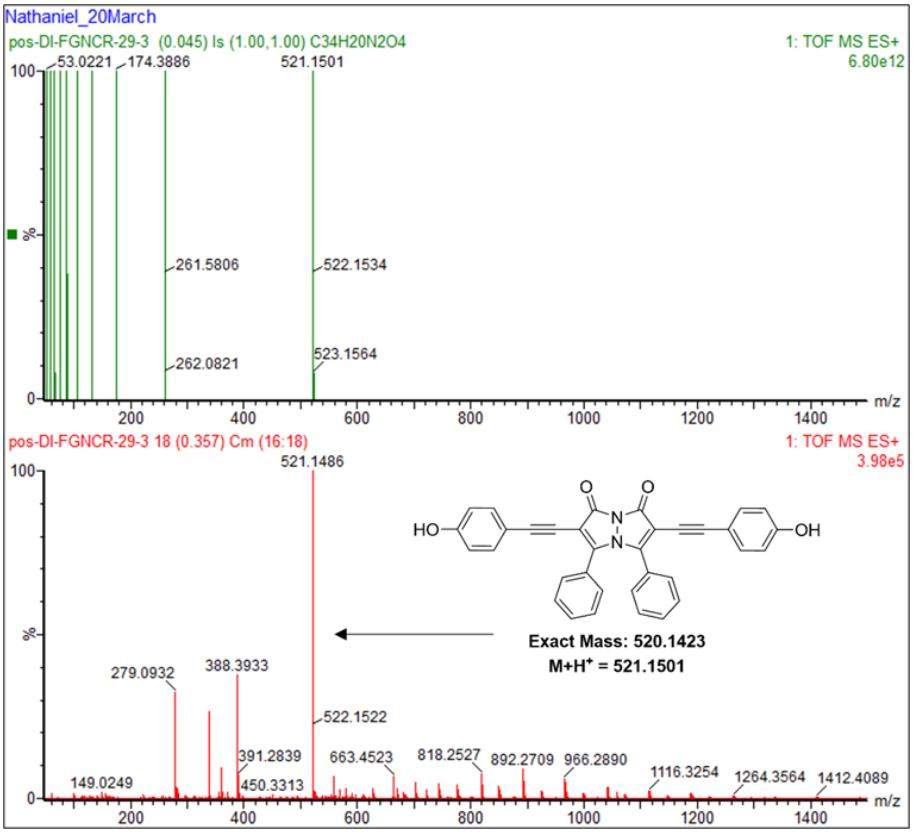

Figure S8. High resolution mass spectrum (HRMS) of compound **2** (top: computationally predicted spectrum; bottom: experimentally-obtained spectrum)

b. *Solution-state experiments*

i. Steady-state UV-visible and fluorescence spectroscopy experiments

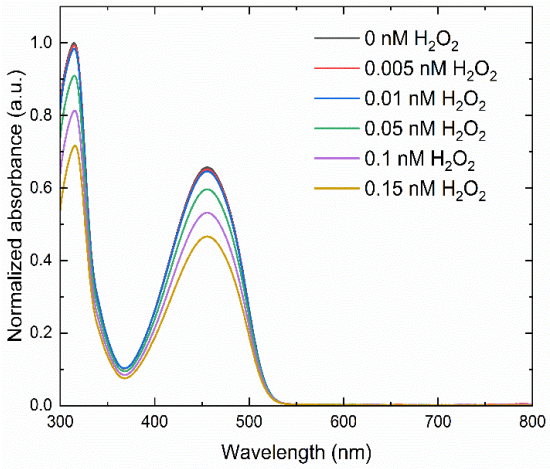

Figure S9. UV-visible spectra of acetonitrile solutions of compound **1** ([**1**] = 10 μM) in the presence of increasing concentrations of hydrogen peroxide

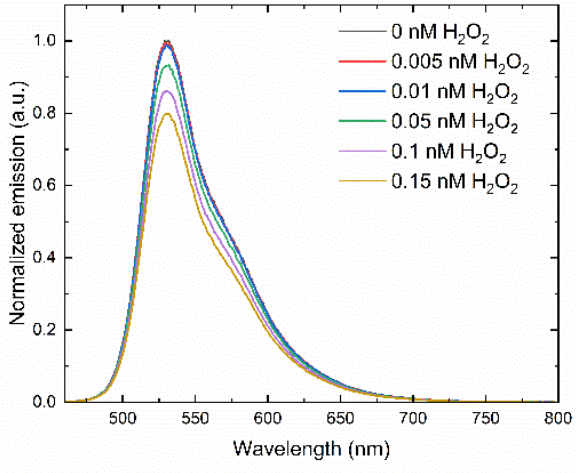

Figure S10. Fluorescence emission spectra of acetonitrile solutions of compound **1** ([**1**] = 10 μM) in the presence of increasing concentrations of hydrogen peroxide

ii. The photophysical responses of compound **1** to H_2O compared to H_2O_2 (high analyte concentrations to enable straightforward visualization of the differences in responses)

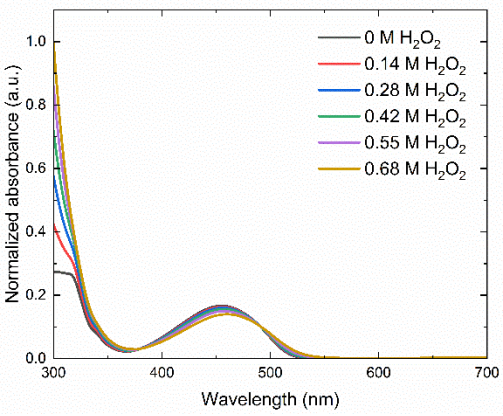

Figure S11. UV-visible absorbance spectra of compound **1** ([**1**] = 10 μM) in the presence of varying concentrations of hydrogen peroxide

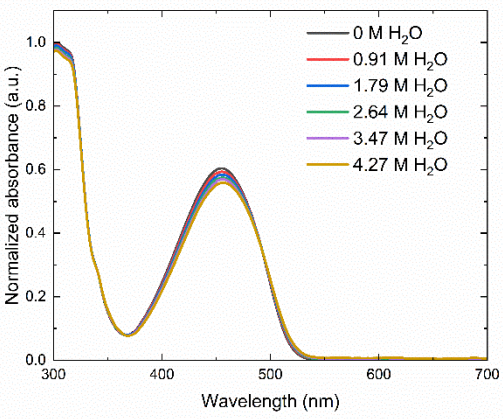

Figure S12. UV-visible absorbance spectra of compound **1** ([**1**] = 10 μM) in the presence of varying concentrations of water

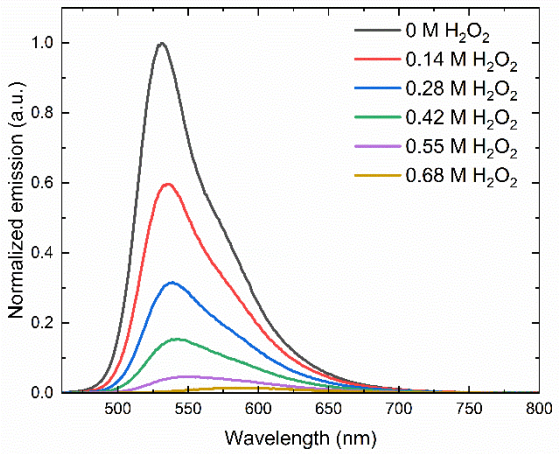

Figure S13. Steady-state fluorescence emission spectra of compound **1** ([**1**] = 10 μM) in the presence of varying concentrations of hydrogen peroxide

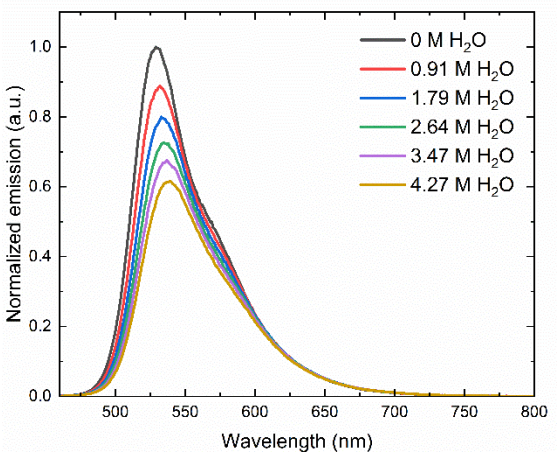

Figure S14. Steady-state fluorescence emission spectra of compound **1** ([**1**] = 10 μM) in the presence of varying concentrations of water

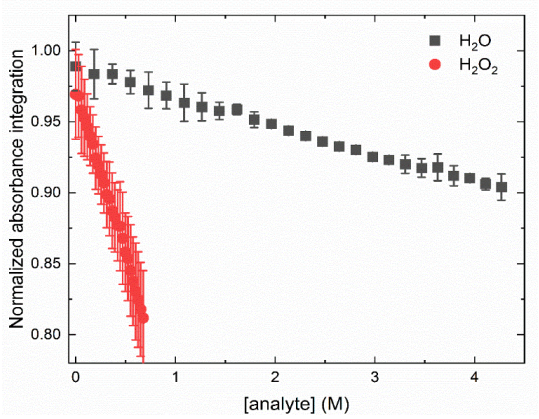

Figure S15. Integration values of absorbance spectra of solutions of compound **1** ([**1**] = 10 μM) (normalized) vs concentration of analyte (H_2O or H_2O_2)

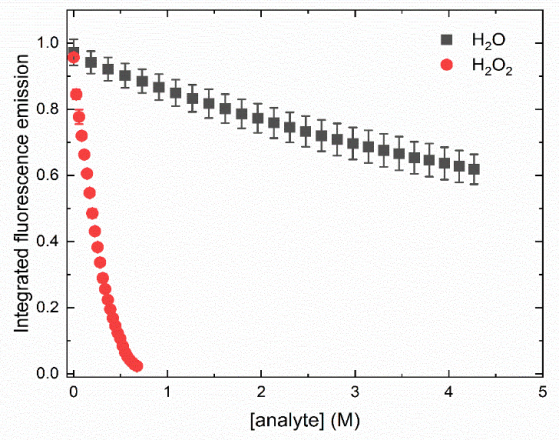

Figure S16. Integration values of fluorescence emission spectra of solutions of compound **1** ([**1**] = 10 μM) (normalized) vs concentration of analyte (H_2O or H_2O_2)

iii. Limit of detection experiments

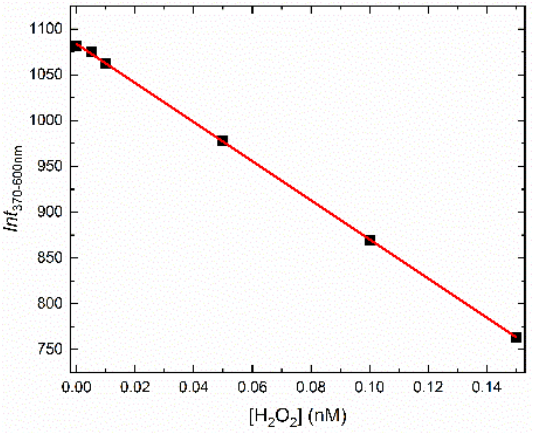

Figure S17. Graphical representation of the effect of increasing hydrogen peroxide concentration on the integrated UV-visible absorbance spectra of solutions of compound **1** ([**1**] = 10 μM in acetonitrile)

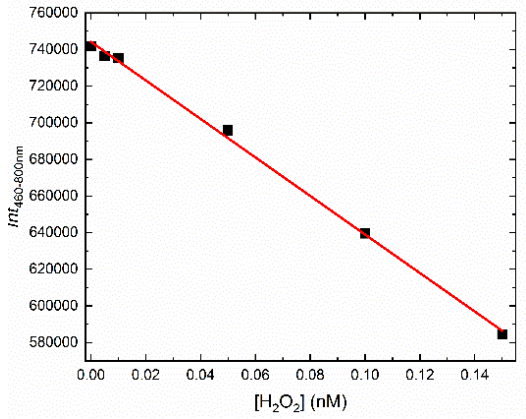

Figure S18. Graphical representation of the effect of increasing hydrogen peroxide concentration on the integrated fluorescence emission spectra of solutions of compound **1** ([**1**] = 10 μM in acetonitrile)

iv. Solution-state colorimetric analysis

H_2O_2 analyte

Ambient lighting:

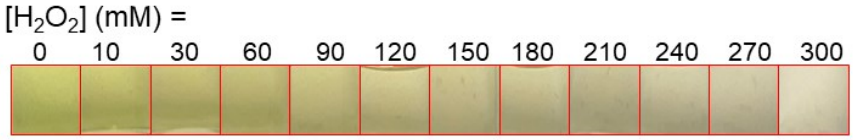

Figure S19. A composite image of solutions of compound **1** after exposure to hydrogen peroxide, viewed under ambient lighting ([**1**] = 10 μM in acetonitrile)

365 nm excitation:

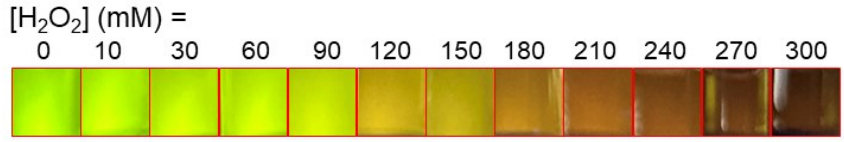

Figure S20. A composite image of solutions of compound **1** after exposure to hydrogen peroxide, viewed under 365 nm excitation ([**1**] = 10 μM in acetonitrile)

H_2O analyte

Ambient lighting:

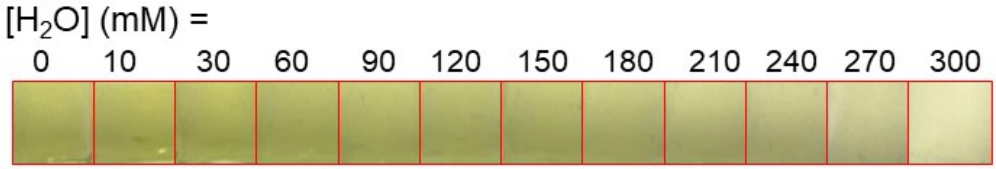

Figure S21. A composite image of solutions of compound **1** after exposure to water, viewed under ambient lighting ([**1**] = 10 μM in acetonitrile)

365 nm excitation:

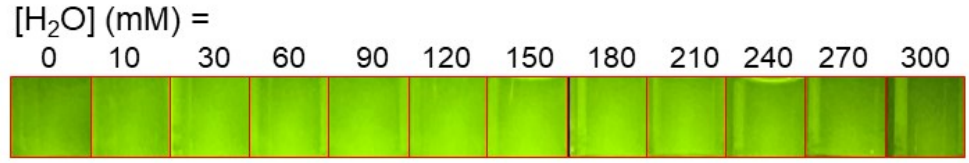

Figure S22. A composite image of solutions of compound **1** after exposure to water, viewed under 365 nm excitation ([**1**] = 10 μM in acetonitrile)

v. Solution-state selectivity experiments

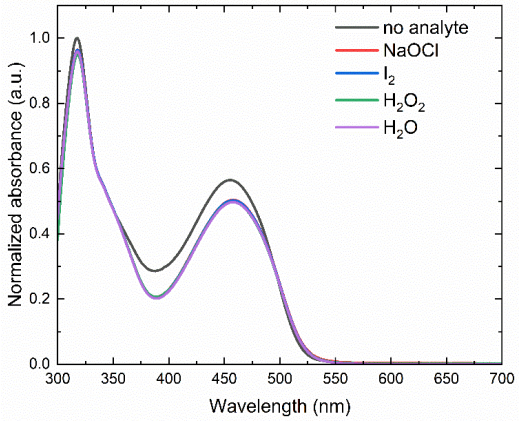

Figure S23. Normalized UV-visible absorbance spectra of acetonitrile solutions of compound **1** after exposure to various analytes ([**1**] = 10 μM; [analyte] = 10 nM)

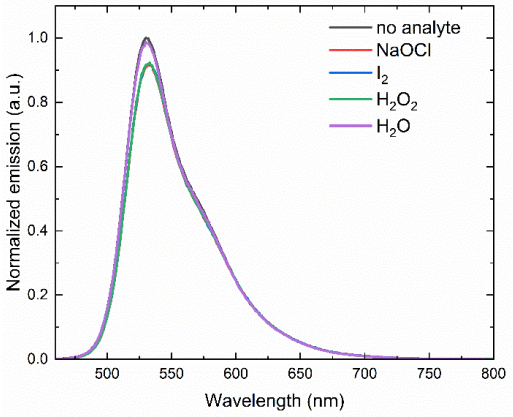

Figure S24. Normalized fluorescence emission spectra of acetonitrile solutions of compound **1** after exposure to various analytes ([**1**] = 10 μM; [analyte] = 10 nM; λ_{ex} = 450 nm)

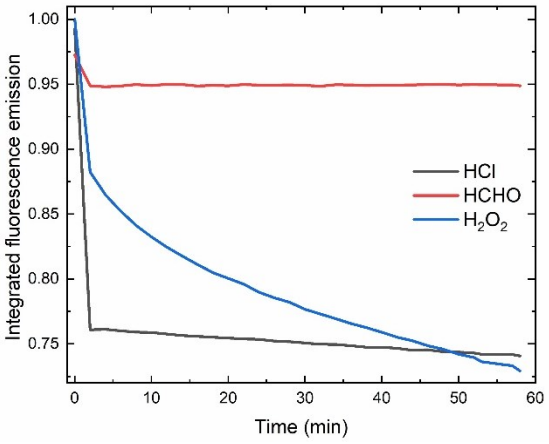

Figure S25. Changes in the fluorescence emission of solutions of compound **1** as a function of time, following exposure to hydrochloric acid (HCl), formaldehyde (HCHO), or hydrogen peroxide (H_2O_2) in Milli-Q tap water ([**1**] = 10 μM; [analyte] = 30 mM)

vi. Real-world solution experiments

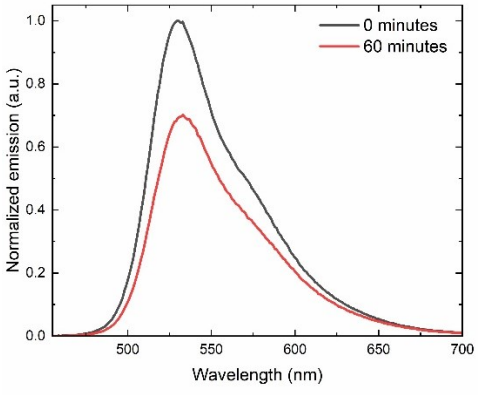

Figure S26. Normalized fluorescence emission of a solution of compound **1** after exposure to hydrogen peroxide in Milli-Q water ([**1**] = 10 μM; [H_2O_2] = 30 mM)

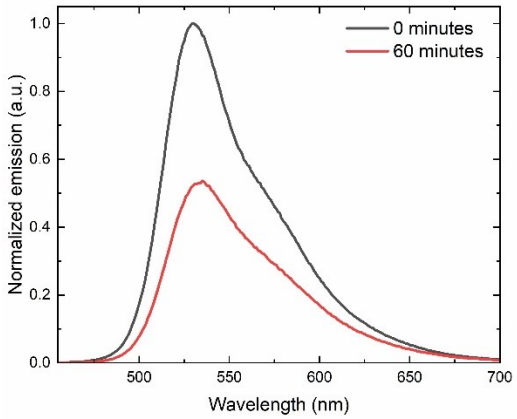

Figure S27. Normalized fluorescence emission of a solution of compound **1** after exposure to hydrogen peroxide in unpurified tap water ([**1**] = 10 μM; [H_2O_2] = 30 mM)

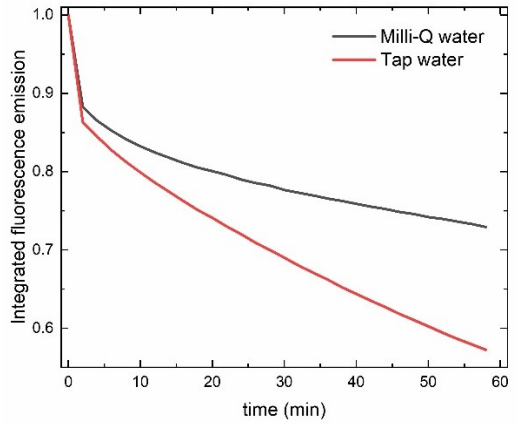

Figure S28. Changes in the fluorescence emission of solutions of compound **1** as a function of time, following exposure to hydrogen peroxide in Milli-Q water or in unpurified tap water ([**1**] = 10 μM; [H_2O_2] = 30 mM)

vii. Kinetics experiments

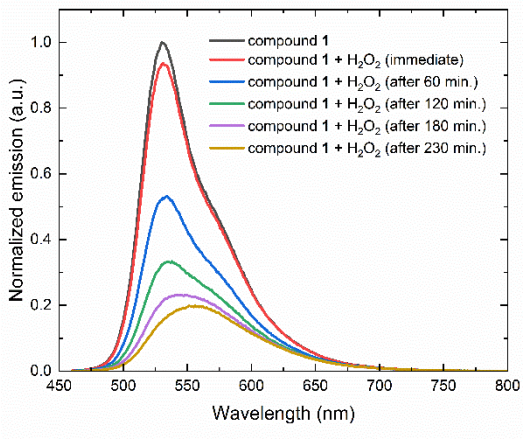

Figure S29. Steady-state fluorescence emission spectra of compound **1** after exposure to H_2O_2, showing the decrease in the fluorescence emission as a function of time

c. *Filter paper-based experiments*

i. Analyte detection in solution using compound **1** – functionalized papers

H_2O_2 analyte

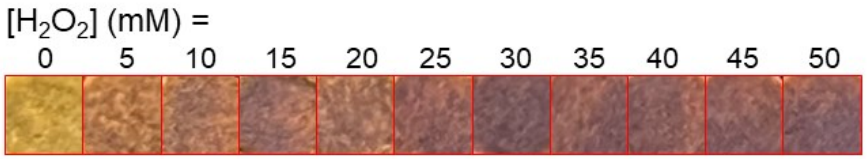

Figure S30. A composite image of Whatman #1 filter paper onto which compound **1** was adsorbed after exposure to hydrogen peroxide, viewed under 365 nm excitation

H_2O analyte

Figure S31. A composite image of Whatman #1 filter paper onto which compound **1** was adsorbed after exposure to water, viewed under 365 nm excitation

ii. Vapor-phase analyte detection using compound **1** – functionalized papers

Figure S32. A composite image of Whatman #1 filter paper onto which compound **1** was adsorbed after exposure to H_2O_2 vapors, viewed under 365 nm excitation

iii. Vapor-phase selectivity studies using compound **1** – functionalized papers

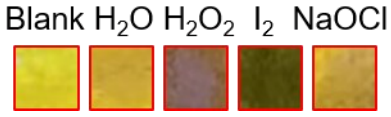

Figure S33. Compound **1** – functionalized filter papers after exposure to vapors of various analytes, photographed under 365 nm excitation

iv. Assessment of reversibility of compound **1** – functionalized papers

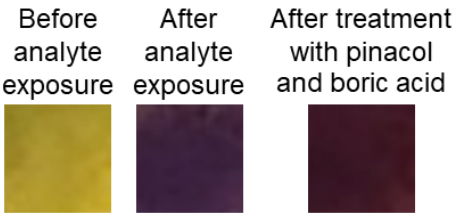

Figure S34. Photographs taken under 365 nm excitation of compound **1** – functionalized papers before analyte exposure, after exposure to H_2O_2, and after treatment with pinacol and boric acid, showing that this treatment does not regenerate the fluorescence of the original compound **1** – functionalized papers

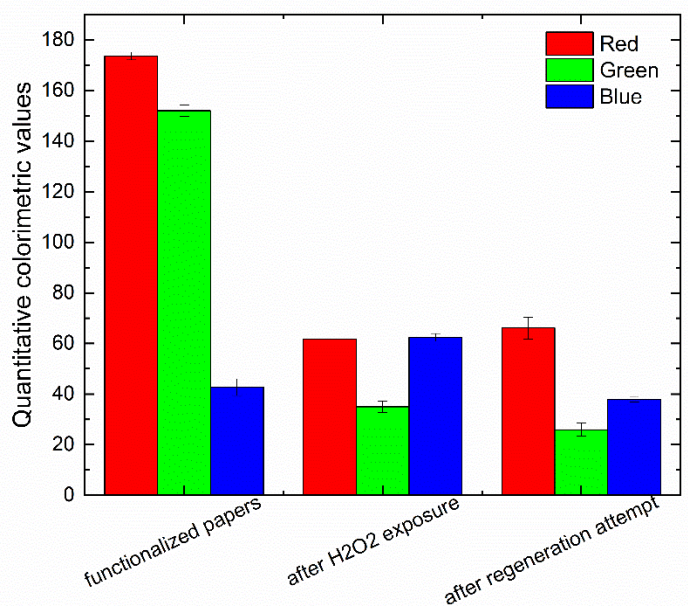

Figure S35. Graphical depiction of the quantitative colorimetric values of compound **1** – functionalized papers before analyte exposure, after exposure to H_2O_2, and after attempts to regenerate the functionalized papers via treatment with pinacol and boric acid

d. <u>High resolution mass spectrometry experiments</u>

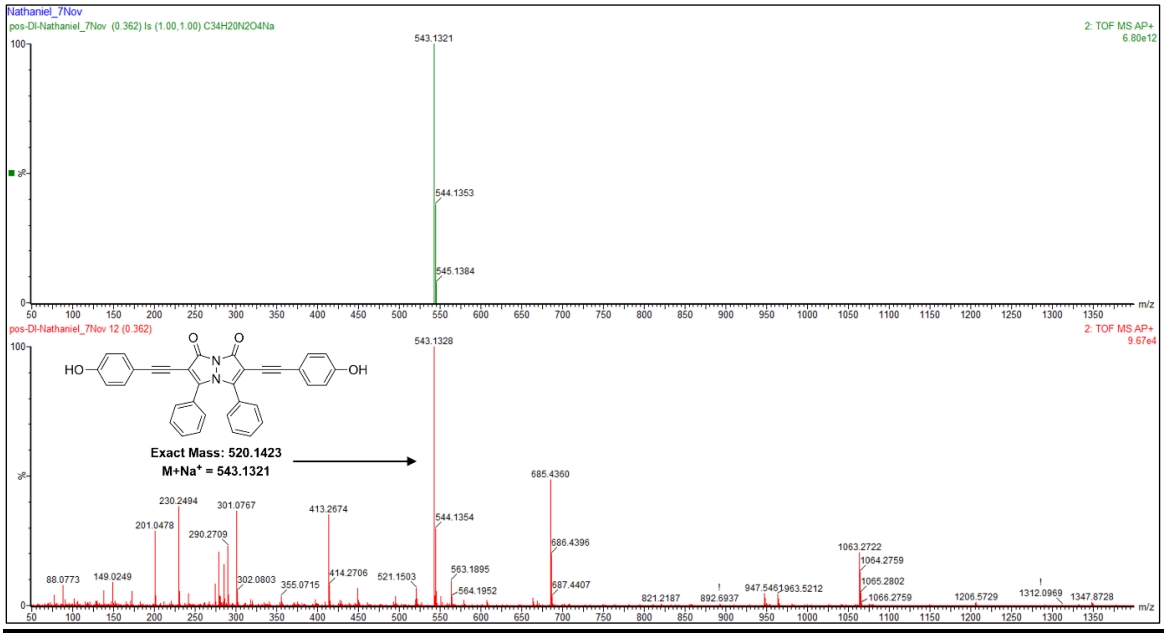

Figure S36. High resolution mass spectrum obtained after mixing compound **1** in a 1:1 mixture of acetonitrile and 30% H_2O_2, showing a mass signal that corresponds to the mass of the compound **2** (top: mass spectrum calculated in the presence of sodium cations; bottom: experimentally-obtained mass spectrum)

e. *[1]H NMR titration experiments*

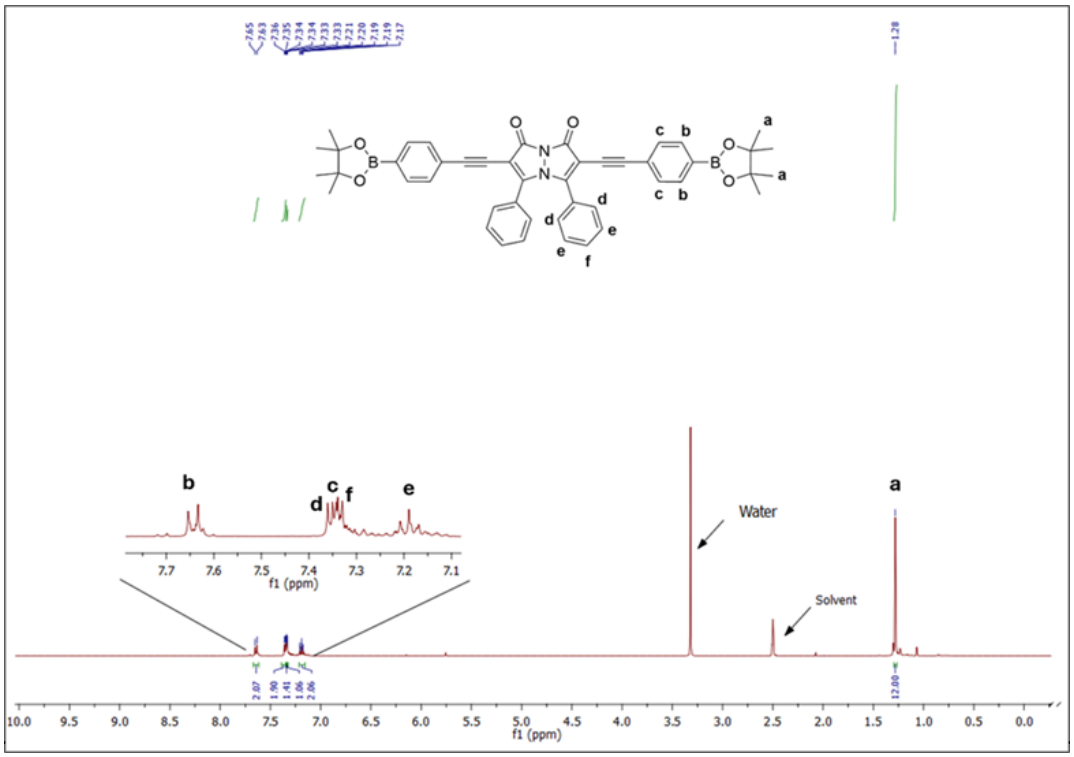

Figure S37. [1]H NMR of compound **1** in DMSO-d_6

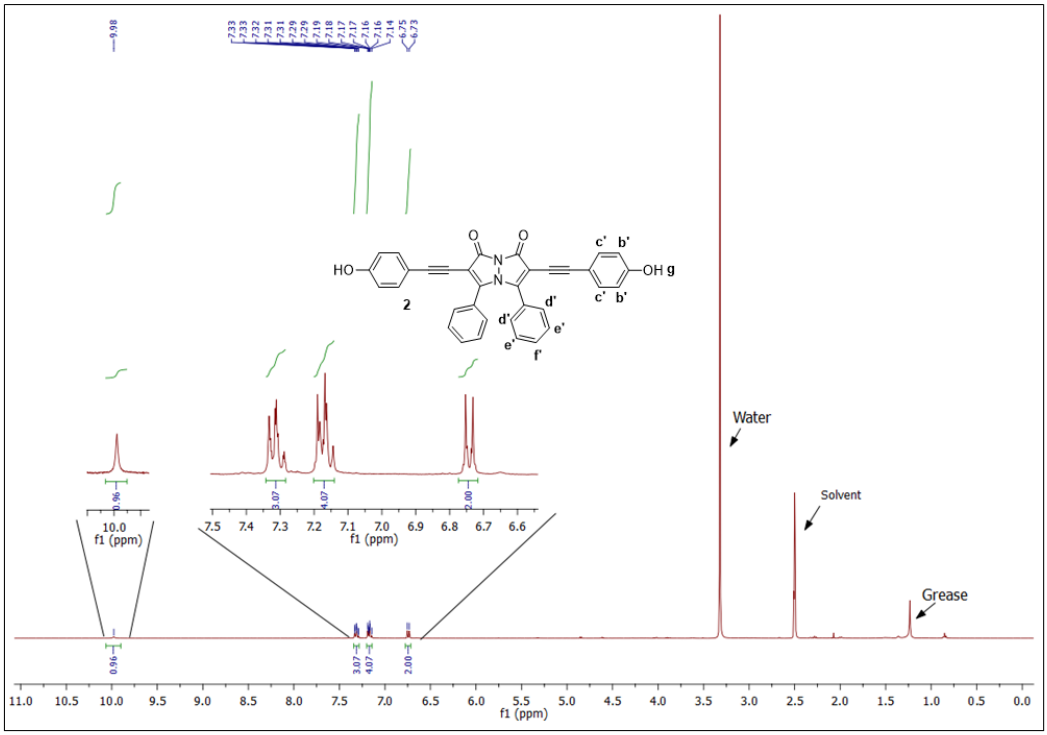

Figure S38. [1]H NMR spectrum of compound **2** in DMSO-d_6

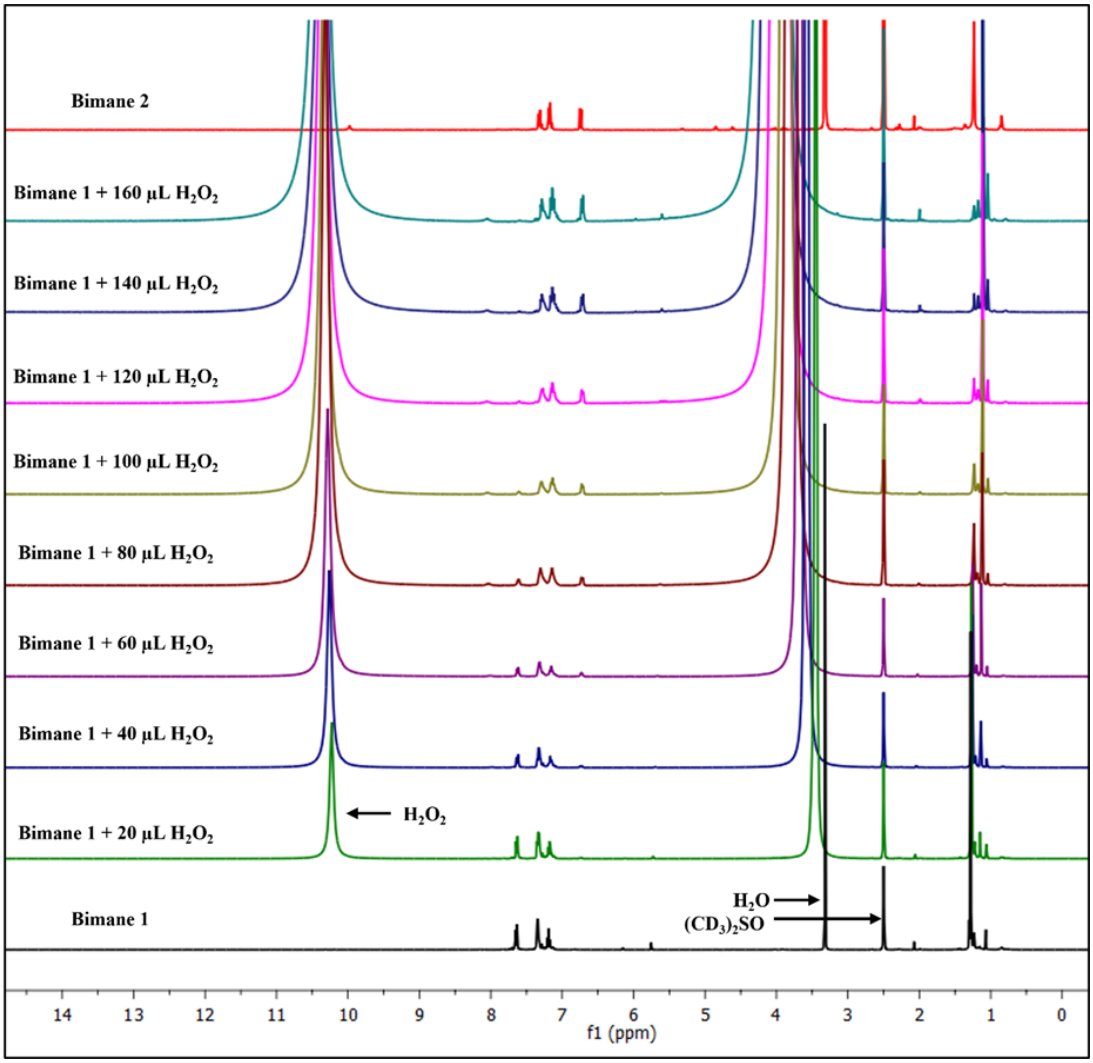

Figure S39. ^{1}H NMR spectra of compound **1** upon the addition of H_2O_2 (30% (w/v), 8.8 M) (0-160 µL, in 20 µL increments), compared to the ^{1}H NMR spectrum of compound **2** (top-most spectrum)

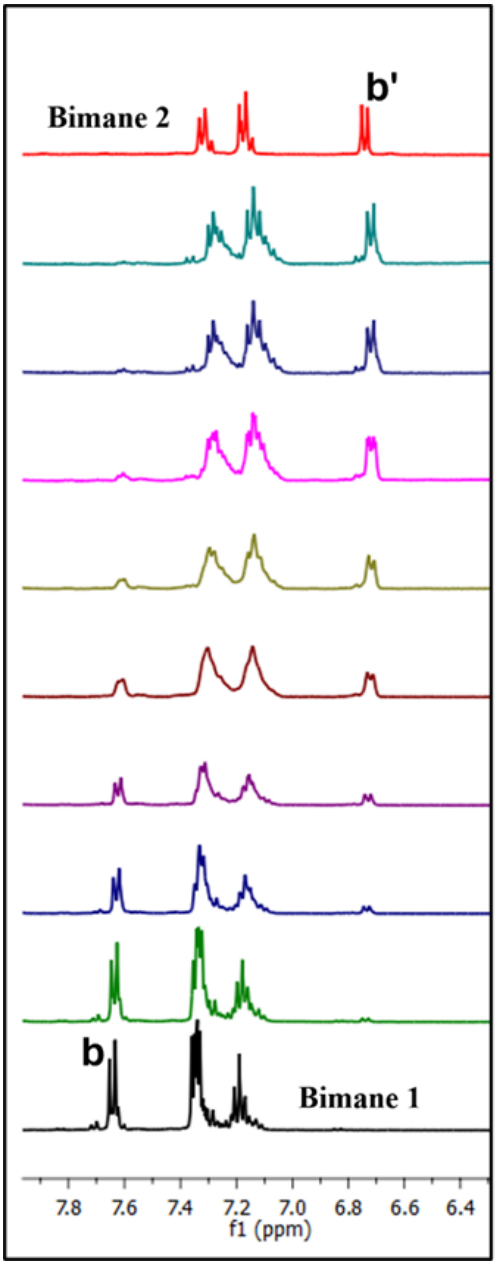

Figure S40. Aromatic region of the ^{1}H NMR spectra of compound **1** upon the addition of H_2O_2 (30% (w/v), 8.8 M) (0-160 µL, in 20 µL increments), compared to the aromatic region of the ^{1}H NMR spectrum of compound **2** (top-most spectrum)

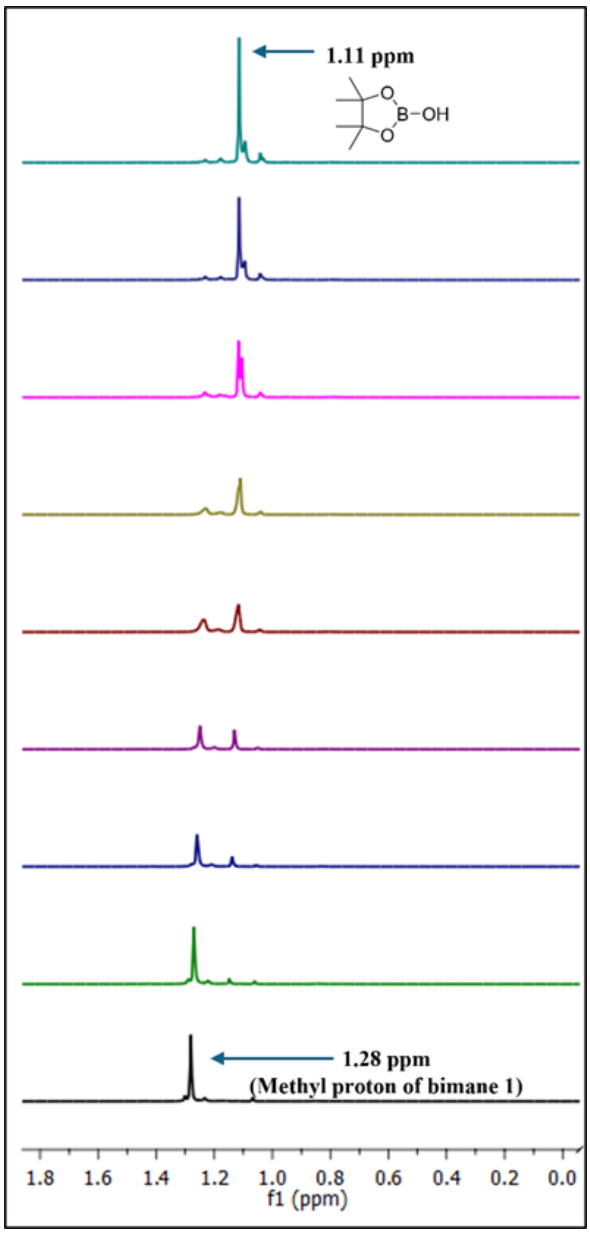

Figure S41. Aliphatic region of the ^{1}H NMR spectra of compound **1** in DMSO-d_6 upon the addition of H_2O_2 (30% (w/v), 8.8 M) (0-160 µL, in 20 µL increments), compared to the ^{1}H NMR spectrum of compound **1** without any H_2O_2 (bottom-most spectrum)

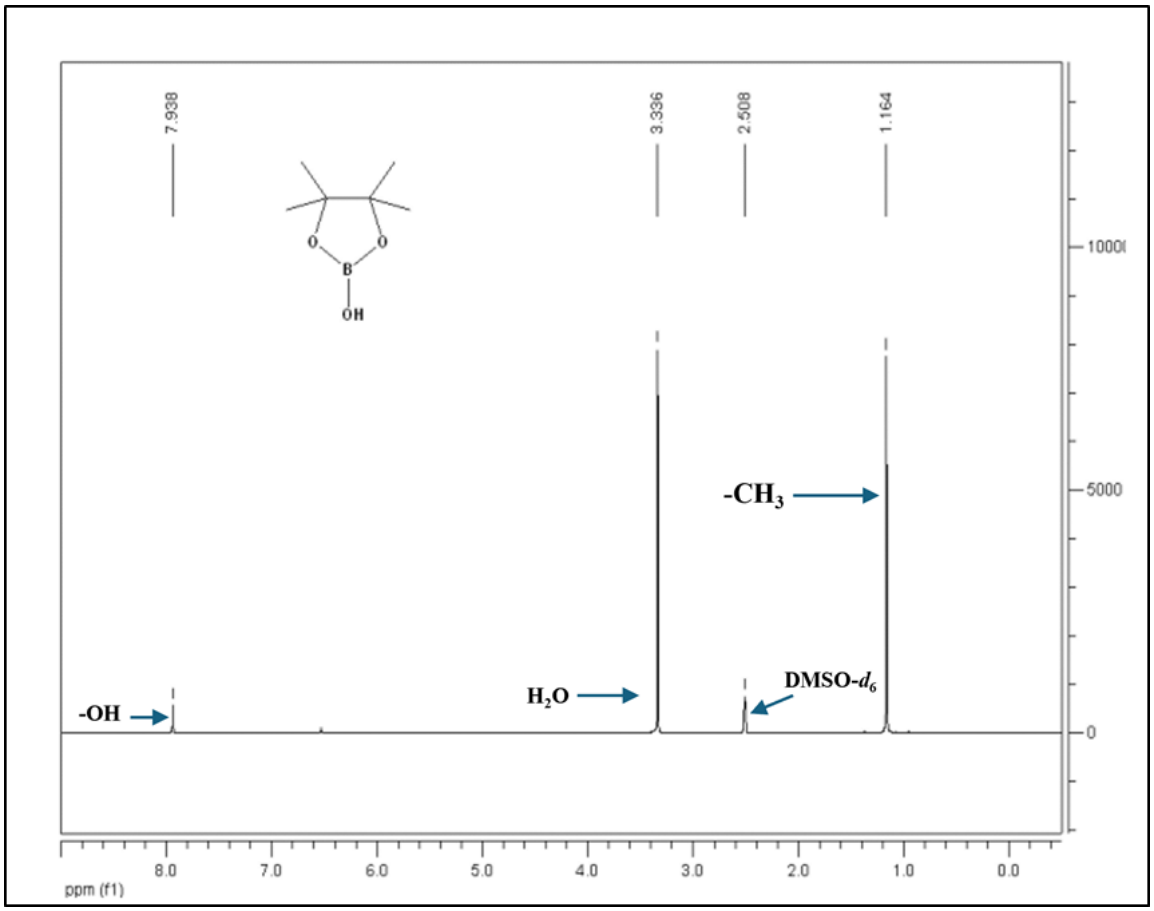

Figure S42. Literature-reported ^{1}H NMR spectrum of boric acid pinacol ester in DMSO-d_6, used for comparison with the spectra acquired during the ^{1}H NMR titration experiments[13]

f. REFERENCES

[1] Szumski, O.; Karmakar, J.; Grynszpan, F. Re-Enter the *syn*-(Me,I)Bimane: A Gateway to Bimane Derivatives with Extended π-Systems. *Synlett.* **2021**, *32*, 1141-1145; DOI: 10.1055/s-0040-1706045.

[2] Lakowicz, J. Principles of Fluorescence Spectroscopy, Third Edition.; Springer: New York USA, **2006**.

[3] Brouwer, A. M. Standards for Photoluminescence Quantum Yield Measurements in Solution (IUPAC Technical Report*). Pure Appl. Chem.* **2011**, *83*, 2213-2228; DOI: 10.1351/PAC-REP-10-09-31.

[4] O'Sullivan, D. W.; Lee, M. Y.; Noone, B. C.; Heikes, B. G. Henry's Law Constant Determinations for Hydrogen Peroxide, Methyl Hydroperoxide, Hydroxymethyl Hydroperoxide, Ethyl Hydroperoxide, and Peroxyacetic Acid. *J. Phys. Chem*. **1996**, *100*, 3241-3247; DOI: 10.1021/jp951168n.

[5] Liu, J.; Bo, X.; Zhao, Z.; Guo, L. Highly Exposed Pt Nanoparticles Supported on Porous Graphene for Electrochemical Detection of Hydrogen Peroxide in Living Cells. *Biosensors Bioelectronics* **2015**, *74*, 71-77; DOI: 10.1016/j.bios.2015.06.042.

[6] Zhang, W.; Ma, D.; Du, J. Prussian Blue Nanoparticles as Peroxidase Mimetics for Sensitive Colorimetric Detection of Hydrogen Peroxide and Glucose. *Talanta* **2014**, *120*, 362-367; DOI: 10.1016/j.talanta.2013.12.028.

[7] Chang, J.; Li, H.; Hou, T.; Duan, W.; Li, F. Paper-Based Fluorescent Sensor via Aggregation Induced Emission Fluorogen for Facile and Sensitive Visual Detection of Hydrogen Peroxide and Glucose. *Biosensors Bioelectronics* **2018**, *104*, 152-157; DOI: 10.1016/j.bios.2018.01.007.

[8] Yeh, I.-H.; Tadepalli, S.; Liu, K.-K. Au@Ag Nanostructures for the Sensitive Detection of Hydrogen Peroxide. *Sci. Reports* **2022**, *12*, 19661; DOI: 10.1038/s41598-022-24344-w.

[9] Niu, Q.; Bao, C.; Cao, X.; Liu, C.; Wang, H.; Lu, W. Ni–Fe PBA Hollow Nanocubes as Efficient Electrode Materials for Highly Sensitive Detection of Guanine and Hydrogen Peroxide in Human Whole Saliva. *Biosensors Bioelectronics* **2019**, *141*, 111445; DOI: 10.1016/j.bios.2019.111445.

[10] Liang, X.; Xu, X.; Qiao, D.; Yin, Z.; Shang, L. Dual Mechanism of an Intramolecular Charge Transfer (ICT)–FRET-Based Fluorescent Probe for the Selective Detection of Hydrogen Peroxide. *Chem. Asian J.* **2017**, *12*, 3187-3194; DOI: 10.1002/asia.201701382.

[11] Tian, R.; Zhang, B.; Zhao, M.; Ma, Q.; Qi, Y. Polyoxometalates as Promising Enzyme Mimics for the Sensitive Detection of Hydrogen Peroxide by Fluorometric Method. *Talanta* **2018**, *188*, 332-338; DOI: 10.1016/j.talanta.2018.05.085.

[12] Han, J.; Chu, C.; Cao, G.; Mao, W.; Wang, S.; Zhao, Z.; Gao, M.; Ye, H.; Xu, X. A Simple Boronic Acid-Based Fluorescent Probe for Selective Detection of Hydrogen Peroxide in Solutions and Living Cells. *Bioorg. Chem.* **2018**, *81*, 362-366; DOI: 10.1016/j.bioorg.2018.08.036.

[13] Cao, S.; Christiansen, R.; Peng, X. Substituent Effects on Oxidation-Induced Formation of Quinone Methides from Arylboronic Ester Precursors. *Chem. – Eur. J.* **2013**, *19*, 9050-9058; DOI: 10.1002/chem.201300539.